Electron-phonon quantum kinetics for spatially inhomogeneous excitations

M. Herbst, M. Glanemann, V. M. Axt, and T. Kuhn
Institut für Festkörpertheorie, Westfälische Wilhelms-Universität, Wilhelm-Klemm-Str. 10, D-48149 Münster, Germany
(Received 12 November 2002; published 6 May 2003)

The dynamics of optically generated carriers interacting with longitudinal optical phonons in spatially inhomogeneous systems is analyzed on a quantum kinetic level. A microscopic density-matrix theory is formulated accounting for arbitrary spatial inhomogeneities in the semiconductor structure and the excitation conditions. The physical origin of the various contributions entering the dynamical equations is discussed. The theory is applied to the dynamics of a wave packet optically generated locally in a quantum wire. We study quantum kinetic features due to the interaction with phonons in the expansion process both in a one-band and a two-band model as well as the generation and dynamics of coherent phonon amplitudes.

DOI: 10.1103/PhysRevB.67.195305 PACS number(s): 73.63.Nm, 78.47.+p, 72.20.Dp

I. INTRODUCTION

On femtosecond time scales a Boltzmann-like description of scattering processes occurring instantaneously between states with well-defined energy is no more adequate. Instead, a quantum kinetic approach has to be used which takes into account energy-time uncertainty but also features like correlation effects between initial and final states in a scattering process and a mutual influence between different interaction mechanisms. A variety of such phenomena has been investigated in the past decade both theoretically and experimentally like the time-dependent broadening of phonon replicas,[1–5] phonon quantum beats,[1,2,6–8] the coherent control of phonon quantum beats and dephasing times,[9–11] phonon scattering between Coulomb-renormalized states,[12,13] quantum kinetics of Coulomb scattering processes,[14–16] plasmons and the buildup of screening,[17–21] and phonon-plasmon coupling.[22]

Besides this enduring reduction in time scales, modern techniques like near-field optical microscopy[23] lead to a continuous decrease in spatial scales accessible by optical experiments. Optical resolutions down to less than 40 nm have already been achieved[24] so that also the assumption of a scattering process occurring at a well-defined position between well-defined momentum states inherent in the scattering term of the Boltzmann equation is losing its validity. Recently, the combination of ultrashort length and time scales has become a field of growing interest. Different techniques have been used to obtain a spatial resolution below the diffraction limit, in particular the near-field optical microscope,[25–29] a solid immersion lens,[30,31] or the excitation and detection through small metallic apertures.[32–34] Here, subjects of the theoretical analysis have been the interaction of the carrier system with the electromagnetic field of the near-field tip[35] as well as the role of Coulomb and electron phonon interaction for the spatial transport of locally created carriers and excitons.[36,37] In these studies, however, scattering processes have been treated on a semiclassical (Markovian) level.

In this contribution we will extend the density-matrix approach to carrier-phonon quantum kinetics which has been successfully used in the past for homogeneous systems[2,5,11,38,39] to systems involving spatial inhomogeneities. These inhomogeneities may be either due to a spatial structure of the sample under consideration or due to an inhomogeneous excitation leading to space-dependent carrier distributions. While in a spatially homogeneous system the **k** space provides a natural representation because of momentum conservation, in spatially inhomogeneous systems there is no such *a priori* distinction of a basis. Here we will derive the theory in a **k**-space representation because in this way it is the natural extension of the homogeneous theory. Other bases, however, are equally possible. Among the variety of other representations we will discuss in some detail the Wigner representation because of (i) its closest similarity with semiclassical kinetics, (ii) its wide usage in quantum transport theory, and (iii) its suitability for a physical interpretation of the terms entering the theory. While on the quantum kinetic level the dynamics is still completely independent of the basis and therefore the choice of the basis is merely a question of convenience, this independence is lost when applying the Markov (semiclassical) approximation. This approximation requires the selection of slowly varying variables which are typically different in different representations. We will discuss this point in detail by comparing the Markov approximations in the **k**-space and the Wigner representation.

In the second part of the paper we will then apply the theory to the dynamics of carriers excited by means of a short laser pulse in a one-dimensional (1D) quantum wire model. The wire geometry is chosen mainly for technical reasons because of the high numerical complexity. Most of the phenomena discussed are not particular for 1D systems and therefore they should all be present also in systems of higher dimension. First we analyze the role of a homogeneous static electric field for the carrier-phonon scattering dynamics, the intracollisional field effect, as an example for the mutual influences between different interactions. Here, strong analogies are revealed between the field effect on phonon scattering and its influence on carrier generation by light absorption, where the field gives rise to the Franz-Keldysh effect. Then we will study the dynamics of a locally generated electronic wave packet both in real and momentum space which will allow us to extract the role of energy-time uncertainty for the spatial dynamics of the wave packet. Finally we will discuss the generation of coherent optical

phonons due to the space charges created by a electronic wave packets. We analyze the dynamics of the resulting lattice polarization as well as its feedback on the electronic subsystem.

The paper is organized as follows: In Sec. II we present the physical model and derive the general theoretical framework in the **k**-space representation (Sec. II A). In Sec. II B the important limiting case of a homogeneous electric field, i.e., the intracollisional field effect is discussed. Section II C is devoted to the formulation of the theory for an inhomogeneous system in terms of a Wigner representation and in Sec. II D we show how different assumptions on temporal and spatial scales lead to different Markov limits. Section III presents numerical results where we discuss in particular the dynamics in a static homogeneous field (Sec. III A), the dynamics of locally generated wave packets (Sec. III B), the creation of coherent phonons (Sec. III C), and the feedback of coherent phonons on the carrier dynamics (Sec. III D). Finally in Sec. IV we will draw some conclusions.

II. THEORY

A. Density-matrix theory for spatially inhomogeneous systems

Most physical variables which are directly related to observables of the charge-carrier system like charge densities, current densities, optical polarizations, distribution functions, etc. are single-particle quantities. The central variable which contains all information for the calculation of such quantities is the single-particle density matrix. In a crystalline solid this density matrix can be separated into intraband and interband contributions. Here we will restrict ourselves to a two-band model of an undoped semiconductor treated in the electron-hole picture. A generalization to a larger number of bands is straightforward. In the two-band case the single-particle density matrix of the carrier system in a crystal momentum (**k**-space) representation consists of the electron density matrix f^e, the hole density matrix f^h, and the interband density matrix p defined as

$$f^e_{\mathbf{k}',\mathbf{k}}=\langle c^\dagger_{\mathbf{k}'}c_{\mathbf{k}}\rangle, \tag{1a}$$

$$f^h_{\mathbf{k}',\mathbf{k}}=\langle d^\dagger_{\mathbf{k}'}d_{\mathbf{k}}\rangle, \tag{1b}$$

$$p_{\mathbf{k}',\mathbf{k}}=\langle d_{-\mathbf{k}'}c_{\mathbf{k}}\rangle, \tag{1c}$$

where $c^\dagger_{\mathbf{k}}$ and $d^\dagger_{\mathbf{k}}$ ($c_{\mathbf{k}}$ and $d_{\mathbf{k}}$) describe the creation (annihilation) of an electron and a hole with momentum **k**, respectively. In the homogeneous case, which has been widely studied in the past, the variables are diagonal, i.e., only the components with $\mathbf{k}=\mathbf{k}'$ are nonzero and they can be directly interpreted as electron and hole distribution functions or the momentum components of the interband polarization.

As for the electronic subsystem, the information on the state of the phonon system is contained in reduced phonon density matrices. Being, however, a Bose system where the particle number is not conserved, also expectation values of an odd number of operators are possible. Thus the lowest order is given by the mean phonon amplitude

$$B_{\mathbf{q}}=\langle b_{\mathbf{q}}\rangle, \tag{2}$$

where $b_{\mathbf{q}}$ denotes the annihilation operator of a phonon with wave vector **q**; $b^\dagger_{\mathbf{q}}$ is the corresponding creation operator. The phonon amplitude is directly related to a mean displacement of the lattice atomes and thus in the case of acoustic phonons to a coherent sound wave and in the case of longitudinal optical (LO) phonons in a polar semiconductor, which will only be considered here, to a lattice polarization,[40]

$$\mathbf{P}_{\mathrm{Ph}}(\mathbf{r})=\frac{\varepsilon_0}{e}\gamma_{\mathrm{Ph}}\sum_{\mathbf{q}}\frac{\mathbf{q}}{q}[e^{i\mathbf{q}\cdot\mathbf{r}}B_{\mathbf{q}}+e^{-i\mathbf{q}\cdot\mathbf{r}}B^*_{\mathbf{q}}], \tag{3}$$

where

$$\gamma_{\mathrm{Ph}}=\sqrt{\frac{2\pi e^2\hbar\omega_{LO}}{\mathcal{V}}\frac{1}{4\pi\varepsilon_0}\left(\frac{1}{\varepsilon_\infty}-\frac{1}{\varepsilon_s}\right)}. \tag{4}$$

ε_s and ε_∞ are the static and optical dielectric constants, respectively, ε_0 is the absolute dielectric constant of the vacuum, ω_{LO} is the phonon frequency, and $\mathcal{V}$ is a normalization volume. In a homogeneous system only a $\mathbf{q}=0$ polarization is possible which, however, often is absent for symmetry reasons. Therefore coherent phonons are usually not considered in that case.

The phonon analog of the single-particle density matrices for the electronic system is conveniently defined as

$$n_{\mathbf{q}',\mathbf{q}}=\langle(b^\dagger_{\mathbf{q}'}-B^*_{\mathbf{q}'})(b_{\mathbf{q}}-B_{\mathbf{q}})\rangle=\langle b^\dagger_{\mathbf{q}'}b_{\mathbf{q}}\rangle-B^*_{\mathbf{q}'}B_{\mathbf{q}}. \tag{5}$$

Its diagonal elements describe the mean occupation number of incoherent phonons in a phonon mode **q** or, equivalently, the fluctuation of the corresponding phonon amplitude, while the off-diagonal elements give rise to space-dependent phonon distributions.

The single-particle part of the Hamiltonian of our system can be decomposed as follows. First, there are the kinetic energies of electrons and holes $\epsilon^e_{\mathbf{k}}$ and $\epsilon^h_{\mathbf{k}}$ in the respective bands. The carriers move in space-dependent potentials which are given by the spatial profiles of the conduction $[V^C(\mathbf{r})]$ and valence $[V^V(\mathbf{r})]$ band edge profiles. These profiles are determined by the material composition in a heterostructure. In low dimensional systems they can be also given by spatial variations of the confinement potential as, e.g., in the case of *V*- or *T*-shaped quantum wires. The fields due to these internal potentials are complemented by externally applied electromagnetic fields. For the purpose of the present study we will consider in particular a combination of two external contributions, a static or temporally slowly varying homogeneous field and the optical field of a laser pulse. By applying the usual dipole approximation based on the assumptions that the fields are sufficiently slowly varying on the length scale of the lattice constant, the corresponding single-particle Hamiltonian is the direct generalization of the standard Hamiltonian used in semiconductor optics for homogeneous systems,

$$H^c=\sum_{\mathbf{k},\mathbf{k}'}\left[(\epsilon^e_{\mathbf{k}}\delta_{\mathbf{k},\mathbf{k}'}+V^e_{\mathbf{k}-\mathbf{k}'})c^\dagger_{\mathbf{k}'}c_{\mathbf{k}}+(\epsilon^h_{\mathbf{k}}\delta_{\mathbf{k},\mathbf{k}'}+V^h_{\mathbf{k}-\mathbf{k}'})d^\dagger_{\mathbf{k}'}d_{\mathbf{k}}\right.$$
$$-\mathbf{M}_{(1/2)(\mathbf{k}+\mathbf{k}')}\cdot\mathbf{E}_{\mathbf{k}-\mathbf{k}'}c^\dagger_{\mathbf{k}'}d^\dagger_{-\mathbf{k}}$$
$$\left.-\mathbf{M}^*_{(1/2)(\mathbf{k}+\mathbf{k}')}\cdot\mathbf{E}^*_{\mathbf{k}-\mathbf{k}'}d_{-\mathbf{k}}c_{\mathbf{k}'}\right], \tag{6}$$

where

$$V^{e,h}_{\mathbf{q}}=\frac{1}{\mathcal{V}}\int e^{-i\mathbf{q}\cdot\mathbf{r}}\ V^{e,h}(\mathbf{r})d^3r \tag{7}$$

denote the Fourier transforms of the space dependent electron and hole potentials,

$$V^e(\mathbf{r},t)=V^C(\mathbf{r})+e\mathbf{E}(\mathbf{r},t)\cdot\mathbf{r}, \tag{8a}$$

$$V^h(\mathbf{r},t)=-V^V(\mathbf{r})-e\mathbf{E}(\mathbf{r},t)\cdot\mathbf{r}, \tag{8b}$$

$\mathbf{E}_{\mathbf{q}}(t)$ is the spatial Fourier transform of the external electric field $\mathbf{E}(\mathbf{r},t)$,

$$\mathbf{M}_{\mathbf{k}}=-e\int_{\mathcal{V}_c}d^3r u^*_{c\mathbf{k}}(\mathbf{r})\mathbf{r}u_{v\mathbf{k}}(\mathbf{r}) \tag{9}$$

is the interband dipole matrix element with $u_{c\mathbf{k}}$ ($u_{v\mathbf{k}}$) denoting the lattice periodic Bloch functions of the conduction (valence) band, and $\mathcal{V}_c$ is the volume of an elementary cell.

The Hamiltonian given above can be formally derived starting from the usual Coulomb gauge by applying the Power-Zienau-Woolley transformation.[41,42] This results in an interaction Hamiltonian which can be expressed completely in terms of the fields **E** and **B**. However, the resulting interaction Hamiltonian is in general nonlocal. A local interaction is obtained by applying the dipole approximation which is well satisfied if the fields are sufficiently slowly varying on the length scale of an elementary cell. Under the same condition the magnetic field contribution of the interaction with the laser field is negligible because it is of the same order as the electric quadrupole contribution. This leads then to the Hamiltonian given by Eq. (6).

Finally, the free-phonon Hamiltonian is given by

$$H^p=\sum_{\mathbf{q}}\hbar\omega_{LO}b^\dagger_{\mathbf{q}}b_{\mathbf{q}}. \tag{10}$$

These parts of the Hamiltonian represent energies corresponding to noninteracting carriers and phonons. As in any genuine many-body system they have to be complemented by interaction terms. The central interaction mechanism for the problems addressed in this paper is the interaction between carriers and LO phonons provided by the Fröhlich coupling. It is described by the Hamiltonian[40]

$$H^{cp}=\sum_{\mathbf{k},\mathbf{q}}\left[g_{\mathbf{q}}c^\dagger_{\mathbf{k}+\mathbf{q}}b_{\mathbf{q}}c_{\mathbf{k}}+g^*_{\mathbf{q}}c^\dagger_{\mathbf{k}}b^\dagger_{\mathbf{q}}c_{\mathbf{k}+\mathbf{q}}-g_{\mathbf{q}}d^\dagger_{\mathbf{k}+\mathbf{q}}b_{\mathbf{q}}d_{\mathbf{k}}\right.$$
$$\left.-g^*_{\mathbf{q}}d^\dagger_{\mathbf{k}}b^\dagger_{\mathbf{q}}d_{\mathbf{k}+\mathbf{q}}\right] \tag{11}$$

with the Fröhlich coupling matrix element $g_{\mathbf{q}}=i\gamma_{\mathrm{Ph}}/q$. In addition, the carriers interact among themselves by means of the Coulomb potential which gives rise to the Hamiltonian

$$H^{cc}=\sum_{\mathbf{k},\mathbf{k}',\mathbf{q}}v_{\mathbf{q}}\left[\frac{1}{2}c^\dagger_{\mathbf{k}}c^\dagger_{\mathbf{k}'}c_{\mathbf{k}'+\mathbf{q}}c_{\mathbf{k}-\mathbf{q}}+\frac{1}{2}d^\dagger_{\mathbf{k}}d^\dagger_{\mathbf{k}'}d_{\mathbf{k}'+\mathbf{q}}d_{\mathbf{k}-\mathbf{q}}\right.$$
$$\left.-c^\dagger_{\mathbf{k}}d^\dagger_{\mathbf{k}'}d_{\mathbf{k}'+\mathbf{q}}c_{\mathbf{k}-\mathbf{q}}\right] \tag{12}$$

with the Coulomb matrix element $v_{\mathbf{q}}=e^2/(\mathcal{V}\varepsilon_0\varepsilon_\infty q^2)$. Here, we have taken into account only the long-range contributions which are the most important ones for typical phenomena studied in this paper. Since the aim of this paper is to study the electron-phonon quantum kinetics, we will disregard carrier-carrier scattering processes but we will take into account the Coulomb interaction on the mean-field (Hartree-Fock) level, which is obtained from Eq. (12) by its mean-field counterpart.

The main task of a kinetic theory is now to set up equations of motion for the dynamical variables defined above. The only equation which is closed within the set of kinetic variables introduced so far is the equation for the coherent phonon amplitude

$$\frac{\partial}{\partial t}B_{\mathbf{q}}=-i\omega_{LO}\ B_{\mathbf{q}}-\frac{i}{\hbar}g^*_{\mathbf{q}}\sum_{\mathbf{k}}\left[f^e_{\mathbf{k},\mathbf{k}+\mathbf{q}}-f^h_{\mathbf{k},\mathbf{k}+\mathbf{q}}\right]. \tag{13}$$

For the other variables, in particular for all electronic density matrices, however, there is no closed set of equations in a many-body system and suitable approximation schemes have to be set up. In a density-matrix approach this consists in introducing higher-order density matrices as new variables and truncating the hierarchy at a certain level. Here we will concentrate on electron-phonon quantum kinetics and include the next level of the phonon-induced branch of the hierarchy. The corresponding variables are phonon-assisted density matrices. Four different variables appear in a two-band model; in the present case they are conveniently introduced according to

$$s^e_{\mathbf{k}',\mathbf{q},\mathbf{k}}=\frac{i}{\hbar}g_{\mathbf{q}}\langle c^\dagger_{\mathbf{k}'}(b_{\mathbf{q}}-B_{\mathbf{q}})c_{\mathbf{k}}\rangle, \tag{14a}$$

$$s^h_{\mathbf{k}',\mathbf{q},\mathbf{k}}=-\frac{i}{\hbar}g_{\mathbf{q}}\langle d^\dagger_{\mathbf{k}'}(b_{\mathbf{q}}-B_{\mathbf{q}})d_{\mathbf{k}}\rangle, \tag{14b}$$

$$t^{(+)}_{\mathbf{k}',\mathbf{q},\mathbf{k}}=\frac{i}{\hbar}g_{\mathbf{q}}\langle d_{-\mathbf{k}'}(b_{\mathbf{q}}-B_{\mathbf{q}})c_{\mathbf{k}}\rangle, \tag{14c}$$

$$t^{(-)}_{\mathbf{k}',\mathbf{q},\mathbf{k}}=-\frac{i}{\hbar}g^*_{\mathbf{q}}\langle d_{-\mathbf{k}'}(b^\dagger_{\mathbf{q}}-B^*_{\mathbf{q}})c_{\mathbf{k}}\rangle. \tag{14d}$$

Since electron-electron interaction via the Coulomb matrix element $v_{\mathbf{q}}$ is taken into account on a mean-field level it does not give rise to new variables. If the phonon hierarchy is truncated by factorization on the level of four-point density matrices, the dynamics of the carrier-phonon system is described by the equations of motion for the single-particle density matrices of the carriers,

$$\frac{\partial}{\partial t} f^e_{\mathbf{k}',\mathbf{k}} = \frac{i}{\hbar} \sum_{\mathbf{k}''} [\mathcal{E}^e_{\mathbf{k}',\mathbf{k}''} f^e_{\mathbf{k}'',\mathbf{k}} - f^e_{\mathbf{k}',\mathbf{k}''} \mathcal{E}^e_{\mathbf{k}'',\mathbf{k}} + \mathcal{U}^*_{\mathbf{k}'',\mathbf{k}'} p_{\mathbf{k}'',\mathbf{k}} - p^*_{\mathbf{k}'',\mathbf{k}'} \mathcal{U}_{\mathbf{k}'',\mathbf{k}}] + \sum_{\mathbf{q}} [s^e_{\mathbf{k}'+\mathbf{q},\mathbf{q},\mathbf{k}} + s^{e*}_{\mathbf{k}+\mathbf{q},\mathbf{q},\mathbf{k}'} - s^e_{\mathbf{k}',\mathbf{q},\mathbf{k}-\mathbf{q}} - s^{e*}_{\mathbf{k},\mathbf{q},\mathbf{k}'-\mathbf{q}}], \tag{15a}$$

$$\frac{\partial}{\partial t} f^h_{\mathbf{k}',\mathbf{k}} = \frac{i}{\hbar} \sum_{\mathbf{k}''} [\mathcal{E}^h_{\mathbf{k}',\mathbf{k}''} f^h_{\mathbf{k}'',\mathbf{k}} - f^h_{\mathbf{k}',\mathbf{k}''} \mathcal{E}^h_{\mathbf{k}'',\mathbf{k}} + \mathcal{U}^*_{-\mathbf{k}',-\mathbf{k}''} p_{-\mathbf{k},-\mathbf{k}''} - p^*_{-\mathbf{k}',-\mathbf{k}''} \mathcal{U}_{-\mathbf{k},-\mathbf{k}''}] + \sum_{\mathbf{q}} [s^h_{\mathbf{k}'+\mathbf{q},\mathbf{q},\mathbf{k}} + s^{h*}_{\mathbf{k}+\mathbf{q},\mathbf{q},\mathbf{k}'} - s^h_{\mathbf{k}',\mathbf{q},\mathbf{k}-\mathbf{q}} - s^{h*}_{\mathbf{k},\mathbf{q},\mathbf{k}'-\mathbf{q}}], \tag{15b}$$

$$\frac{\partial}{\partial t} p_{\mathbf{k}',\mathbf{k}} = \frac{i}{\hbar} \sum_{\mathbf{k}''} [-\mathcal{E}^h_{-\mathbf{k}'',-\mathbf{k}'} p_{\mathbf{k}'',\mathbf{k}} - p_{\mathbf{k}',\mathbf{k}''} \mathcal{E}^e_{\mathbf{k}'',\mathbf{k}} + \mathcal{U}_{\mathbf{k}',\mathbf{k}''} f^e_{\mathbf{k}'',\mathbf{k}} - \mathcal{U}_{\mathbf{k}'',\mathbf{k}} (\delta_{\mathbf{k}',\mathbf{k}''} - f^h_{-\mathbf{k}'',-\mathbf{k}'})] + \sum_{\mathbf{q}} [t^{(+)}_{\mathbf{k}'+\mathbf{q},\mathbf{q},\mathbf{k}} - t^{(-)}_{\mathbf{k}'-\mathbf{q},\mathbf{q},\mathbf{k}} - t^{(+)}_{\mathbf{k}',\mathbf{q},\mathbf{k}-\mathbf{q}} + t^{(-)}_{\mathbf{k}',\mathbf{q},\mathbf{k}+\mathbf{q}}], \tag{15c}$$

the equation of motion for the density matrix of incoherent phonons,

$$\frac{\partial}{\partial t} n_{\mathbf{q}',\mathbf{q}} = \frac{g_{\mathbf{q}'}}{g_{\mathbf{q}}} \sum_{\mathbf{k}} [s^e_{\mathbf{k}+\mathbf{q}',\mathbf{q},\mathbf{k}} + s^h_{\mathbf{k}+\mathbf{q}',\mathbf{q},\mathbf{k}}] + \frac{g^*_{\mathbf{q}}}{g^*_{\mathbf{q}'}} \sum_{\mathbf{k}} [s^{e*}_{\mathbf{k}+\mathbf{q},\mathbf{q}',\mathbf{k}} + s^{h*}_{\mathbf{k}+\mathbf{q},\mathbf{q}',\mathbf{k}}], \tag{16}$$

and the equations for the phonon-assisted density matrices, e.g.,

$$\begin{aligned}\frac{\partial}{\partial t} s^e_{\mathbf{k}',\mathbf{q},\mathbf{k}} = \frac{i}{\hbar} \sum_{\mathbf{k}''} & [\mathcal{E}^e_{\mathbf{k}',\mathbf{k}''} s^e_{\mathbf{k}'',\mathbf{q},\mathbf{k}} - s^e_{\mathbf{k}',\mathbf{q},\mathbf{k}''} \mathcal{E}^e_{\mathbf{k}'',\mathbf{k}} - f^e_{\mathbf{k}',\mathbf{k}''} \tilde{s}^e_{\mathbf{k}'',\mathbf{q},\mathbf{k}} + \tilde{s}^e_{\mathbf{k}',\mathbf{q},\mathbf{k}''} f^e_{\mathbf{k}'',\mathbf{k}}] - i\omega_{LO} s^e_{\mathbf{k}',\mathbf{q},\mathbf{k}} \\ & + \frac{i}{\hbar} \sum_{\mathbf{k}''} [\mathcal{U}^*_{\mathbf{k}'',\mathbf{k}'} t^{(+)}_{\mathbf{k}'',\mathbf{q},\mathbf{k}} - \mathcal{U}_{\mathbf{k}'',\mathbf{k}} t^{(-)*}_{\mathbf{k}'',\mathbf{q},\mathbf{k}'} - p^*_{\mathbf{k}'',\mathbf{k}'} \tilde{t}^{(+)}_{\mathbf{k}'',\mathbf{q},\mathbf{k}} + p_{\mathbf{k}'',\mathbf{k}} \tilde{t}^{(-)*}_{\mathbf{k}'',\mathbf{q},\mathbf{k}'}] + \frac{1}{\hbar^2} \sum_{\mathbf{k}'',\mathbf{q}'} g_{\mathbf{q}} g^*_{\mathbf{q}'} [(\delta_{\mathbf{q}',\mathbf{q}} \\ & + n_{\mathbf{q}',\mathbf{q}}) f^e_{\mathbf{k}',\mathbf{k}''+\mathbf{q}'} (\delta_{\mathbf{k}'',\mathbf{k}} - f^e_{\mathbf{k}'',\mathbf{k}}) - n_{\mathbf{q}',\mathbf{q}} (\delta_{\mathbf{k}',\mathbf{k}''+\mathbf{q}'} - f^e_{\mathbf{k}',\mathbf{k}''+\mathbf{q}'}) f^e_{\mathbf{k}'',\mathbf{k}} - \delta_{\mathbf{q}',\mathbf{q}} p^*_{\mathbf{k}''+\mathbf{q}',\mathbf{k}'} p_{\mathbf{k}'',\mathbf{k}}].\end{aligned} \tag{17}$$

The equations for s^h and $t^{(\pm)}$ have the same structure as for s^e. The single-particle part and the mean-field Coulomb contribution is contained in the intra- and interband energy matrices

$$\mathcal{E}^{e,h}_{\mathbf{k}',\mathbf{k}} = \epsilon^{e,h}_{\mathbf{k}} \delta_{\mathbf{k}',\mathbf{k}} + V^{e,h}_{\mathbf{k}-\mathbf{k}'} \pm [g_{\mathbf{k}-\mathbf{k}'} B_{\mathbf{k}-\mathbf{k}'} + g^*_{\mathbf{k}'-\mathbf{k}} B^*_{\mathbf{k}'-\mathbf{k}}] \pm v_{\mathbf{k}'-\mathbf{k}} \sum_{\mathbf{q}} [f^e_{\mathbf{k}'+\mathbf{q},\mathbf{k}+\mathbf{q}} - f^h_{\mathbf{k}'+\mathbf{q},\mathbf{k}+\mathbf{q}}] - \sum_{\mathbf{q}} v_{\mathbf{q}} f^{e,h}_{\mathbf{k}'+\mathbf{q},\mathbf{k}+\mathbf{q}}, \tag{18a}$$

$$\mathcal{U}_{\mathbf{k}',\mathbf{k}} = -\mathbf{M}_{(1/2)(\mathbf{k}'+\mathbf{k})} \cdot \mathbf{E}_{\mathbf{k}-\mathbf{k}'}(t) - \sum_{\mathbf{q}} v_{\mathbf{q}} p_{\mathbf{k}'+\mathbf{q},\mathbf{k}+\mathbf{q}}, \tag{18b}$$

where the upper sign in Eq. (18a) refers to electrons and the lower sign to holes. The various contributions have the following origin: The first term in Eq. (18a) is the single-particle energy $\epsilon_{\mathbf{k}}$, the second term is due to an internal and external single-particle potential $V^e(\mathbf{r})$ which is the result, e.g., of band gap variations in heterostructures or an externally applied electric field; the third term results from polarization charges associated with coherent phonons; the fourth term (Hartree term) is the induced potential due to a local charge nonequilibrium between electrons and holes; and the last term (Fock term) denotes the exchange energy resulting in a band gap renormalization which is in general space dependent. In Eq. (18b) the first term describes the coupling to a classical electric field with the spatial Fourier component $\mathbf{E}_{\mathbf{k}}$ treated in dipole approximation with the interband dipole matrix element $\mathbf{M}_{\mathbf{k}}$, and the second term is the interband Fock part responsible for excitonic effects and the Coulomb enhancement of interband transitions. These terms are obtained if already from the onset the full carrier-carrier Hamiltonian [Eq. (12)] is replaced by the corresponding mean-field Hamiltonian. If the full Hamiltonian is taken for the derivation of the equations of motion for the phonon-assisted density matrices and the factorization is performed afterwards there appear additional terms describing Coulomb renormalizations of the carrier-phonon interaction processes according to[12,13]

$$\tilde{s}^{e,h}_{\mathbf{k}',\mathbf{q},\mathbf{k}} = -\sum_{\mathbf{q}'} v_{\mathbf{q}'} s^{e,h}_{\mathbf{k}'+\mathbf{q}',\mathbf{q},\mathbf{k}+\mathbf{q}'} \pm v_{\mathbf{k}'-\mathbf{k}} \sum_{\mathbf{q}'} [s^e_{\mathbf{k}'+\mathbf{q}',\mathbf{q},\mathbf{k}+\mathbf{q}'} + s^h_{\mathbf{k}'+\mathbf{q}',\mathbf{q},\mathbf{k}+\mathbf{q}'}], \tag{19a}$$

$$\tilde{t}^{(\pm)}_{\mathbf{k}',\mathbf{q},\mathbf{k}} = -\sum_{\mathbf{q}'} v_{\mathbf{q}'} t^{(\pm)}_{\mathbf{k}'+\mathbf{q}',\mathbf{q},\mathbf{k}+\mathbf{q}'}. \tag{19b}$$

In particular, Eq. (19b) describes the fact that scattering processes occur between excitonic states and we have shown earlier[12] that in the case of a sufficiently strong electron-phonon coupling and at elevated temperatures they give rise to discrete phonon sidebands of the exciton in the absorption spectrum occurring below the excitonic transition in the gap and a broadened sideband in the continuum above the exciton, which are known from perturbative calculations of linear spectra since a long time ago.[43] For the case of excitation high up in the band, as will be studied in this paper, they

have very little influence on the carrier dynamics,[13] however, they considerably increase the numerical effort, and therefore in the following they will be neglected.

Carrier-phonon scattering processes on the quantum kinetic level are described by the dynamics of the phonon-assisted density matrices. Obviously, the last term on the right-hand side of Eq. (17) has a structure which reminds one of scattering terms in the Boltzmann equation, however, in a nondiagonal generalization. As will be discussed in more detail in Sec. II D the Boltzmann limit is obtained by performing a Markov approximation under the assumption of sufficiently slowly varying functions in space and time. Since in the Boltzmann equation the scattering rates due to different interaction mechanisms simply add up without interference, all contributions to Eq. (17) resulting from other mechanisms than carrier-phonon interaction have to be neglected. This shows that the quantum kinetic treatment, besides the correct treatment of the short time- and length-scale behavior, includes a variety of additional phenomena related to the mutual influence of different mechanisms. In particular, the carrier-phonon scattering dynamics is modified by intra- and interband Fock terms, external fields, band-gap variations, self-consistent (Hartree) fields, and lattice polarizations due to coherent phonons.

B. Homogeneous electric field

The theory developed in the previous section is valid for arbitrary space-dependent external potentials and laser fields. In particular we have seen that also the phonon scattering dynamics which is described by the phonon assisted density matrices is affected by these external potentials. A subject which, because of its great importance for many modern electronic devices, has been studied by various approaches in the past years is the influence of an electric field on the scattering dynamics, a phenomenon which is generally called the *intracollisional field effect*.[3,44–55] In order to get some insight into this problem within our approach let us discuss in this section the theory for the limiting case of a homogeneous electric field in a uniform material. This is the simplest example for an external influence *during* the time it takes to complete phonon scattering events. We assume that the system is homogeneously excited and that all the dynamical variables remain spatially homogeneous. This means that all the single-particle density matrices are diagonal, i.e., $f^e_{\mathbf{k}',\mathbf{k}}=f^e_{\mathbf{k}}\delta_{\mathbf{k}',\mathbf{k}}$, $f^h_{\mathbf{k}',\mathbf{k}}=f^h_{\mathbf{k}}\delta_{\mathbf{k}',\mathbf{k}}$, $p_{\mathbf{k}',\mathbf{k}}=p_{\mathbf{k}}\delta_{\mathbf{k}',\mathbf{k}}$. Due to charge neutrality in the electron-hole system all Hartree-like terms (induced potentials) are absent in this case. Furthermore, only a coherent phonon amplitude with vanishing wave vector B_0 describing a homogeneous lattice polarization is compatible with the assumption of a homogeneous system. Again due to charge neutrality, however, this amplitude is not excited by the dynamics of electrons and holes in the homogeneous case. Therefore coherent phonons will be neglected in the present case.

For a homogeneous electric field the Fourier transforms of the intraband single-particle potentials $V^{e,h}_{\mathbf{q}}$ reduce to differential operators and they are conveniently separated from the intraband energies. Then the resulting equations of motion for the single-particle density matrices read

$$\frac{\partial}{\partial t}f^e_{\mathbf{k}}=\frac{e\mathbf{E}(t)}{\hbar}\cdot\frac{\partial}{\partial\mathbf{k}}f^e_{\mathbf{k}}+\frac{i}{\hbar}[\mathcal{U}^*_{\mathbf{k}}p_{\mathbf{k}}-\mathcal{U}_{\mathbf{k}}p^*_{\mathbf{k}}]+\sum_{\mathbf{q}}2\,\mathrm{Re}[s^e_{\mathbf{k}+\mathbf{q},\mathbf{q},\mathbf{k}}-s^e_{\mathbf{k},\mathbf{q},\mathbf{k}-\mathbf{q}}], \tag{20a}$$

$$\frac{\partial}{\partial t}f^h_{\mathbf{k}}=-\frac{e\mathbf{E}(t)}{\hbar}\cdot\frac{\partial}{\partial\mathbf{k}}f^h_{\mathbf{k}}+\frac{i}{\hbar}[\mathcal{U}^*_{-\mathbf{k}}p_{-\mathbf{k}}-\mathcal{U}_{-\mathbf{k}}p^*_{-\mathbf{k}}]+\sum_{\mathbf{q}}2\,\mathrm{Re}[s^h_{\mathbf{k}+\mathbf{q},\mathbf{q},\mathbf{k}}-s^h_{\mathbf{k},\mathbf{q},\mathbf{k}-\mathbf{q}}], \tag{20b}$$

$$\frac{\partial}{\partial t}p_{\mathbf{k}}=-\frac{i}{\hbar}[\mathcal{E}^e_{\mathbf{k}}+\mathcal{E}^h_{-\mathbf{k}}]p_{\mathbf{k}}+\frac{e\mathbf{E}(t)}{\hbar}\cdot\frac{\partial}{\partial\mathbf{k}}p_{\mathbf{k}}-\frac{i}{\hbar}\mathcal{U}_{\mathbf{k}}[1-f^e_{\mathbf{k}}-f^h_{-\mathbf{k}}]+\sum_{\mathbf{q}}[t^{(+)}_{\mathbf{k}+\mathbf{q},\mathbf{q},\mathbf{k}}-t^{(-)}_{\mathbf{k}-\mathbf{q},\mathbf{q},\mathbf{k}}-t^{(+)}_{\mathbf{k},\mathbf{q},\mathbf{k}-\mathbf{q}}+t^{(-)}_{\mathbf{k},\mathbf{q},\mathbf{k}+\mathbf{q}}], \tag{20c}$$

with the intra- and interband energies given by

$$\mathcal{E}^{e,h}_{\mathbf{k}}=\epsilon^e_{\mathbf{k}}-\sum_{\mathbf{q}}v_{\mathbf{q}}f^{e,h}_{\mathbf{k}+\mathbf{q}}$$

$$\text{and}\quad \mathcal{U}_{\mathbf{k}}=-\mathbf{M}_{\mathbf{k}}\cdot\mathbf{E}(t)-\sum_{\mathbf{q}}v_{\mathbf{q}}p_{\mathbf{k}+\mathbf{q}}. \tag{21}$$

The phonon-assisted density matrices satisfy the following equations of motion:

$$\begin{aligned}\frac{\partial}{\partial t}s^e_{\mathbf{k}',\mathbf{q},\mathbf{k}}&=\frac{i}{\hbar}[\mathcal{E}^e_{\mathbf{k}'}-\mathcal{E}^e_{\mathbf{k}}-\hbar\omega_{LO}]s^e_{\mathbf{k}',\mathbf{q},\mathbf{k}}-\frac{e\mathbf{E}}{\hbar}\cdot\left(\frac{\partial}{\partial\mathbf{k}'}+\frac{\partial}{\partial\mathbf{k}}\right)s^e_{\mathbf{k}',\mathbf{q},\mathbf{k}}\\&+\frac{i}{\hbar}[\mathcal{U}^*_{\mathbf{k}'}t^{(+)}_{\mathbf{k}',\mathbf{q},\mathbf{k}}-\mathcal{U}_{\mathbf{k}}t^{(-)*}_{\mathbf{k},\mathbf{q},\mathbf{k}'}]\\&+\frac{|g_{\mathbf{q}}|^2}{\hbar^2}[(1+n_{\mathbf{q}})f^e_{\mathbf{k}'}(1-f^e_{\mathbf{k}})-n_{\mathbf{q}}f^e_{\mathbf{k}}(1-f^e_{\mathbf{k}'})-p^*_{\mathbf{k}'}p_{\mathbf{k}}]\end{aligned} \tag{22}$$

with $\mathbf{q}=\mathbf{k}'-\mathbf{k}$. This is essentially the same set of equations of motion as in the homogeneous case without field,[2] the homogeneous part in each equation, however, is supplemented by a field term which has the same structure as in the Boltzmann equation giving rise to a drift in $\mathbf{k}$ space. Equations (20a)–(22) are two-band generalizations including mean-field Coulomb contributions of the one-band high-field quantum transport equations which are usually called Levinson equation[44] or Barker-Ferry equation.[45,46] It should be noted that $\mathbf{E}$ here denotes the full external electric field

which in the present case typically consists of two different contributions: the laser field with a frequency in the optical range describing the optical excitation and an additional static or slowly varying (compared to the optical case) field. A close look at the dominant frequency parts of the various dynamical variables reveals that for static and low-frequency fields the drift terms in **k** space are most important while for optical fields the interband coupling $\mathcal{U}$ is dominant. It should be noted, however, that in the presence of very strong fields also the other terms may become relevant. A static field in the interband self-energy gives rise to Zener tunneling and an optical field in the drift terms leads to free-carrier absorption.

The most interesting point now is the fact that the drift terms do not only appear in the equations of motion for the distribution functions, where they are well known from the semiclassical or Boltzmann case, but they also appear in the equations for the polarization and for the phonon-assisted density matrices. The polarization describes the light-induced dynamics; the presence of a field term modifies the corresponding processes like, e.g., light absorption where it gives rise to the Franz-Keldysh effect. The phonon assisted density matrices describe the phonon-induced dynamics, in particular phonon scattering processes. The field terms again modify this dynamics; thus they describe an intracollisional field effect. Both these effects are absent in a Boltzmann approach because there all transition rates are calculated between momentum states of the crystal. In addition, the present treatment reveals the strong symmetry between the effect of the field on the light-induced and phonon-induced dynamics. In this language the Franz-Keldysh effect may be described as an intracollisional field effect of the light absorption process exactly in the same way as the intracollisional field effect of phonon absorption or emission processes.[56] We will come back to this point in Sec. III A when discussing numerical results.

C. Wigner representation

Let us now return to the full spatially inhomogeneous system. While in a homogeneous system the **k**-space representation is distinguished from other bases because here the single-particle density matrices are diagonal, in the absence of translational invariance there is no such *a priori* basis distinction. The laws of quantum mechanics are independent of the choice of a particular basis. The only approximation that has been made in the derivation of the quantum kinetic model in Sec. II A is the truncation of the hierarchy. This truncation is independent of the single-particle basis chosen and therefore the theory is still completely base independent. Also the structure of the equations is very similar in other representations. Therefore the basis can be chosen according to its mathematical or numerical suitability.

There is one representation which is of particular interest both for the physical interpretation of the dynamics and for the comparison with a semiclassical kinetic theory. This is the phase-space representation introduced by Wigner already in 1932.[57] The Wigner function bears the closest similarity with classical distribution functions and all expectation values are calculated in complete analogy to the classical case. In contrast to a distribution function, however, it is not necessarily positive definite and therefore it cannot be interpreted in a probabilistic way. In the context of quantum transport in semiconductor nanostructures like resonant tunneling diodes the Wigner function has been extensively used in the past years.[58–61] In most of these calculations scattering processes have been treated in a simplified way either by using a relaxation time approximation or by using semiclassical scattering rates. Such rates, however, describe scattering processes at a well-defined position between well-defined momentum states and therefore they are not consistent with Heisenberg's uncertainty relation between momentum and position. This problem can be overcome within a quantum kinetic carrier-phonon model which accounts for both energy-time and momentum-position uncertainty in the Wigner representation. An iterative approach where the Wigner function is expanded in terms involving a given number of scattering events has been discussed and applied to the resonant tunneling diode.[62,63] The correlation expansion used in this paper results in a closed set of dynamical equations which, after transformation into the Wigner representation, allows us to identify most clearly temporal and spatial nonlocalities.

The Wigner functions corresponding to the single-particle density matrices are defined as the Fourier transforms of the single-particle density matrices with respect to the relative momentum,

$$\mathcal{F}^{e,h}_{\mathbf{k}}(\mathbf{r}) = \sum_{\mathbf{q}} e^{i\mathbf{q}\cdot\mathbf{r}} f^{e,h}_{\mathbf{k}-(1/2)\mathbf{q},\mathbf{k}+(1/2)\mathbf{q}}, \tag{23a}$$

$$\mathcal{P}_{\mathbf{k}}(\mathbf{r}) = \sum_{\mathbf{q}} e^{i\mathbf{q}\cdot\mathbf{r}} p_{\mathbf{k}-(1/2)\mathbf{q},\mathbf{k}+(1/2)\mathbf{q}}. \tag{23b}$$

From the intraband Wigner function both the distribution in momentum space $f^{e,h}_{\mathbf{k}}$ and the carrier densities in real space $n^{e,h}(\mathbf{r})$ are directly obtained as

$$f^{e,h}_{\mathbf{k}} = \frac{1}{\mathcal{V}} \int d^3r \mathcal{F}^{e,h}_{\mathbf{k}}(\mathbf{r}), \tag{24a}$$

$$n^{e,h}(\mathbf{r}) = \frac{1}{\mathcal{V}} \sum_{\mathbf{k}} \mathcal{F}^{e,h}_{\mathbf{k}}(\mathbf{r}), \tag{24b}$$

and also higher moments are calculated exactly as in the classical case. The electron and hole current densities $\mathbf{j}^{e,h}(\mathbf{r})$ and kinetic energy densities $t^{e,h}(\mathbf{r})$ in the case of parabolic bands are given by

$$\mathbf{j}^{e,h}(\mathbf{r}) = \frac{1}{\mathcal{V}} \sum_{\mathbf{k}} \frac{\hbar\mathbf{k}}{m_{e,h}} \mathcal{F}^{e,h}_{\mathbf{k}}(\mathbf{r}), \tag{25a}$$

$$t^{e,h}(\mathbf{r}) = \frac{1}{\mathcal{V}} \sum_{\mathbf{k}} \frac{\hbar^2\mathbf{k}^2}{2m_{e,h}} \mathcal{F}^{e,h}_{\mathbf{k}}(\mathbf{r}), \tag{25b}$$

and for space points with nonvanishing carrier densities one can define a local drift velocity $\mathbf{v}^{e,h}(\mathbf{r})$ and mean kinetic energy per carrier $E^{e,h}_{\mathrm{kin}}(\mathbf{r})$ according to

$$\mathbf{v}^{e,h}(\mathbf{r}) = \mathbf{j}^{e,h}(\mathbf{r})/n^{e,h}(\mathbf{r}), \tag{26a}$$

$$E^{e,h}_{\rm kin}(\mathbf{r}) = t^{e,h}(\mathbf{r})/n^{e,h}(\mathbf{r}). \tag{26b}$$

From the interband Wigner function the space-dependent macroscopic optical polarization $\mathbf{P}_{\rm opt}(\mathbf{r})$ is obtained according to

$$\mathbf{P}_{\rm opt}(\mathbf{r}) = \frac{1}{\mathcal{V}} \sum_{\mathbf{k}} [\mathbf{M}^*_{\mathbf{k}} \mathcal{P}_{\mathbf{k}}(\mathbf{r}) + \mathbf{M}_{\mathbf{k}} \mathcal{P}^*_{\mathbf{k}}(\mathbf{r})]. \tag{27}$$

It is convenient to transform also the phonon-assisted density matrices into a Wigner representation according to

$$\mathcal{S}^{e,h}_{\mathbf{k},\mathbf{q}}(\mathbf{r}) = \sum_{\mathbf{q}'} e^{i\mathbf{q}'\cdot\mathbf{r}} s^{e,h}_{\mathbf{k}+\mathbf{q}-\frac{1}{2}\mathbf{q}',\mathbf{q},\mathbf{k}+\frac{1}{2}\mathbf{q}'}, \tag{28a}$$

$$\mathcal{T}^{(\pm)}_{\mathbf{k},\mathbf{q}}(\mathbf{r}) = \sum_{\mathbf{q}'} e^{i\mathbf{q}'\cdot\mathbf{r}} t^{(\pm)}_{\mathbf{k}\pm\mathbf{q}-\frac{1}{2}\mathbf{q}',\mathbf{q},\mathbf{k}+\frac{1}{2}\mathbf{q}'}. \tag{28b}$$

Then the equations of motion for the single-particle density matrices can be cast into the compact form,

$$\begin{aligned}\frac{\partial}{\partial t}\mathcal{F}^e_{\mathbf{k}}(\mathbf{r}) = \frac{i}{\hbar}\{&\hat{\mathbf{W}}^{++}[\mathcal{E}^e_{\mathbf{k}}(\mathbf{r})\mathcal{F}^e_{\mathbf{k}}(\mathbf{r})] - \hat{\mathbf{W}}^{++}[\mathcal{F}^e_{\mathbf{k}}(\mathbf{r})\mathcal{E}^e_{\mathbf{k}}(\mathbf{r})] \\ &+ \hat{\mathbf{W}}^{++}[\mathcal{U}^*_{\mathbf{k}}(\mathbf{r})\mathcal{P}_{\mathbf{k}}(\mathbf{r})] - \hat{\mathbf{W}}^{++}[\mathcal{P}^*_{\mathbf{k}}(\mathbf{r})\mathcal{U}_{\mathbf{k}}(\mathbf{r})]\} \\ &+ \sum_{\mathbf{q}} 2\,\mathrm{Re}[\mathcal{S}^e_{\mathbf{k},\mathbf{q}}(\mathbf{r}) - \mathcal{S}^e_{\mathbf{k}-\mathbf{q},\mathbf{q}}(\mathbf{r})],\end{aligned} \tag{29a}$$

$$\begin{aligned}\frac{\partial}{\partial t}\mathcal{F}^h_{\mathbf{k}}(\mathbf{r}) = \frac{i}{\hbar}\{&\hat{\mathbf{W}}^{++}[\mathcal{E}^h_{\mathbf{k}}(\mathbf{r})\mathcal{F}^h_{\mathbf{k}}(\mathbf{r})] - \hat{\mathbf{W}}^{++}[\mathcal{F}^h_{\mathbf{k}}(\mathbf{r})\mathcal{E}^h_{\mathbf{k}}(\mathbf{r})] \\ &+ \hat{\mathbf{W}}^{--}[\mathcal{U}^*_{-\mathbf{k}}(\mathbf{r})\mathcal{P}_{-\mathbf{k}}(\mathbf{r})] - \hat{\mathbf{W}}^{--}[\mathcal{P}^*_{-\mathbf{k}}(\mathbf{r})\mathcal{U}_{-\mathbf{k}}(\mathbf{r})]\} \\ &+ \sum_{\mathbf{q}} 2\,\mathrm{Re}[\mathcal{S}^h_{\mathbf{k},\mathbf{q}}(\mathbf{r}) - \mathcal{S}^h_{\mathbf{k}-\mathbf{q},\mathbf{q}}(\mathbf{r})],\end{aligned} \tag{29b}$$

$$\begin{aligned}\frac{\partial}{\partial t}\mathcal{P}^e_{\mathbf{k}}(\mathbf{r}) = \frac{i}{\hbar}\{&-\hat{\mathbf{W}}^{-+}[\mathcal{E}^h_{-\mathbf{k}}(\mathbf{r})\mathcal{P}_{\mathbf{k}}(\mathbf{r})] - \hat{\mathbf{W}}^{++}[\mathcal{P}_{\mathbf{k}}(\mathbf{r})\mathcal{E}^e_{\mathbf{k}}(\mathbf{r})] \\ &+ \hat{\mathbf{W}}^{++}[\mathcal{U}_{\mathbf{k}}(\mathbf{r})\mathcal{F}^e_{\mathbf{k}}(\mathbf{r})] + \hat{\mathbf{W}}^{-+}[\mathcal{F}^h_{-\mathbf{k}}(\mathbf{r})\mathcal{U}_{\mathbf{k}}(\mathbf{r})]\} \\ &- \frac{i}{\hbar}\mathcal{U}_{\mathbf{k}}(\mathbf{r}) + \sum_{\mathbf{q}} [\mathcal{T}^{(+)}_{\mathbf{k},\mathbf{q}}(\mathbf{r}) - \mathcal{T}^{(-)}_{\mathbf{k},\mathbf{q}}(\mathbf{r}) - \mathcal{T}^{(+)}_{\mathbf{k}-\mathbf{q},\mathbf{q}}(\mathbf{r}) \\ &+ \mathcal{T}^{(-)}_{\mathbf{k}-\mathbf{q},\mathbf{q}}(\mathbf{r})],\end{aligned} \tag{29c}$$

where we have introduced the operator $\hat{\mathbf{W}}^{\sigma\sigma'}$ which is defined by its action on two arbitrary phase-space functions according to

$$\begin{aligned}&\hat{\mathbf{W}}^{\sigma\sigma'}[g_{\mathbf{k}_1}(\mathbf{r}_1)h_{\mathbf{k}_2}(\mathbf{r}_2)] \\ &= \frac{1}{\mathcal{V}^2}\sum_{\mathbf{k}',\mathbf{k}''}\int d^3r'\,d^3r''\,e^{i(\sigma\mathbf{k}''\cdot\mathbf{r}' - \sigma'\mathbf{k}'\cdot\mathbf{r}'')} \\ &\quad\times g_{\mathbf{k}_1+(1/2)\mathbf{k}''}(\mathbf{r}_1+\mathbf{r}'')\;\; h_{\mathbf{k}_2+(1/2)\mathbf{k}'}(\mathbf{r}_2+\mathbf{r}').\end{aligned} \tag{30}$$

Here, σ and σ' can take the values $+1$ or -1. By means of a Taylor expansion this integral operator is formally equivalent to a differential operator of infinite order:

$$\begin{aligned}&\hat{\mathbf{W}}^{\sigma\sigma'}[g_{\mathbf{k}_1}(\mathbf{r}_1)h_{\mathbf{k}_2}(\mathbf{r}_2)] \\ &= \sum_{n,m=0}^{\infty}\frac{(-1)^m i^{n+m}\sigma^n\sigma'^m}{2^{n+m}n!\,m!}\left(\frac{\partial}{\partial\mathbf{k}_1}\cdot\frac{\partial}{\partial\mathbf{r}_2}\right)^n\left(\frac{\partial}{\partial\mathbf{k}_2}\cdot\frac{\partial}{\partial\mathbf{r}_1}\right)^m \\ &\quad\times g_{\mathbf{k}_1}(\mathbf{r}_1)h_{\mathbf{k}_2}(\mathbf{r}_2).\end{aligned} \tag{31}$$

The mean-field part is contained in the intra- and interband energies in Wigner representation,

$$\mathcal{E}^{e,h}_{\mathbf{k}}(\mathbf{r}) = \sum_{\mathbf{q}} e^{i\mathbf{q}\cdot\mathbf{r}}\mathcal{E}^{e,h}_{\mathbf{k}-(1/2)\mathbf{q},\mathbf{k}+(1/2)\mathbf{q}}, \tag{32a}$$

$$\mathcal{U}_{\mathbf{k}}(\mathbf{r}) = \sum_{\mathbf{q}} e^{i\mathbf{q}\cdot\mathbf{r}}\mathcal{U}_{\mathbf{k}-(1/2)\mathbf{q},\mathbf{k}+(1/2)\mathbf{q}}. \tag{32b}$$

The equation of motion for the phonon assisted density matrix $\mathcal{S}^e$ in the Wigner representation reads

$$\begin{aligned}\frac{\partial}{\partial t}\mathcal{S}^e_{\mathbf{k},\mathbf{q}}(\mathbf{r}) = &\frac{i}{\hbar}\{\hat{\mathbf{W}}^{++}[\mathcal{E}^e_{\mathbf{k}+\mathbf{q}}(\mathbf{r})\mathcal{S}^e_{\mathbf{k},\mathbf{q}}(\mathbf{r})] - \hat{\mathbf{W}}^{++}[\mathcal{S}^e_{\mathbf{k},\mathbf{q}}(\mathbf{r})\mathcal{E}^e_{\mathbf{k}}(\mathbf{r})]\} - i\omega_{LO}\mathcal{S}^e_{\mathbf{k},\mathbf{q}}(\mathbf{r}) \\ &+ \frac{i}{\hbar}\{\hat{\mathbf{W}}^{++}[\mathcal{U}^*_{\mathbf{k}+\mathbf{q}}(\mathbf{r})\mathcal{T}^{(+)}_{\mathbf{k},\mathbf{q}}(\mathbf{r})] - \hat{\mathbf{W}}^{++}[\mathcal{T}^{(-)*}_{\mathbf{k},\mathbf{q}}(\mathbf{r})\mathcal{U}_{\mathbf{k}}(\mathbf{r})]\} \\ &- \frac{|g_{\mathbf{q}}|^2}{\hbar^2}(\hat{\mathbf{W}}^{++}[\mathcal{P}^*_{\mathbf{k}+\mathbf{q}}(\mathbf{r})\mathcal{P}_{\mathbf{k}}(\mathbf{r})] - (n_{\mathbf{q}}+1)\hat{\mathbf{W}}^{++}[\mathcal{F}^e_{\mathbf{k}+\mathbf{q}}(\mathbf{r})(1-\mathcal{F}^e_{\mathbf{k}}(\mathbf{r}))] + n_{\mathbf{q}}\hat{\mathbf{W}}^{++}[(1-\mathcal{F}^e_{\mathbf{k}+\mathbf{q}}(\mathbf{r}))\mathcal{F}^e_{\mathbf{k}}(\mathbf{r})])\end{aligned} \tag{33}$$

and the equations for the other phonon-assisted density matrices have the same structure. Here, for reasons of simplicity we have assumed that the distribution of incoherent phonons remains spatially homogeneous, i.e., the corresponding density matrix is diagonal in momentum space: $n_{\mathbf{q}',\mathbf{q}} = n_{\mathbf{q}}\delta_{\mathbf{q}',\mathbf{q}}$. The generalization to space-dependent (off-diagonal) phonon distributions is straightforward. Equations (29a) and (33) describe the dynamics of two-band Wigner functions with

quantum kinetic carrier-phonon scattering. Two-band or multiband Wigner equations without scattering have been discussed previously for single-particle[64] and mean-field[65] Hamiltonians.

In this notation the analogy with the spatially homogeneous case (see Ref. 2) becomes particularly transparent: Simple products of the dynamical variables are replaced by products involving the operator $\hat{\mathbf{W}}^{\sigma\sigma'}$. In the case of spatially homogeneous dynamical variables this operator reduces to the unity operator and the spatially homogeneous set of equations of motion is recovered. For weakly inhomogeneous systems the structure of the drift term in the Boltzmann equation is directly obtained if in all terms involving the intraband self-energies $\mathcal{E}^{e,h}$ only the first-order derivatives in the differential form of $\hat{\mathbf{W}}^{\sigma\sigma'}$ are kept and all higher-order derivatives are assumed to be negligible. Scattering processes where the factors $\mathcal{F}$ and $(1-\mathcal{F})$ are evaluated at the same position result if $\hat{\mathbf{W}}^{\sigma\sigma'}$ is replaced by the unity operator in the source terms for the phonon-assisted density matrices. However, as will be discussed below, this still is not sufficient to obtain spatially local scattering processes as in the Boltzmann picture.

The intra- and interband energy functions have a particularly clear structure in the Wigner representation. They can be written as

$$\mathcal{E}^{e,h}_{\mathbf{k}}(\mathbf{r}) = \epsilon^{e,h}_{\mathbf{k}} + V^{e,h}(\mathbf{r}) - \sum_{\mathbf{q}} v_{\mathbf{q}} \mathcal{F}^{e,h}_{\mathbf{k}-\mathbf{q}}(\mathbf{r}) \mp e\Phi_{\mathrm{sc}}(\mathbf{r}), \tag{34a}$$

$$\mathcal{U}_{\mathbf{k}}(\mathbf{r}) = -\mathbf{M}_{\mathbf{k}} \cdot \mathbf{E}(\mathbf{r}) - \sum_{\mathbf{q}} v_{\mathbf{q}} \mathcal{P}_{\mathbf{k}-\mathbf{q}}(\mathbf{r}), \tag{34b}$$

where the Hartree and coherent phonon terms give rise to the self-consistent electrostatic potential Φ_{sc} determined by the Poisson equation

$$\nabla^2 \Phi_{\mathrm{sc}}(\mathbf{r}) = \frac{e}{\varepsilon_0 \varepsilon_\infty \mathcal{V}} \sum_{\mathbf{k}} [\mathcal{F}^e_{\mathbf{k}}(\mathbf{r}) - \mathcal{F}^h_{\mathbf{k}}(\mathbf{r})] + \frac{1}{\varepsilon_0} \mathrm{div}\, \mathbf{P}_{\mathrm{Ph}}(\mathbf{r}). \tag{35}$$

Thus this potential is created both due to electronic and phononic charges built up by the coupled dynamics of the carrier-phonon system.

Equation (33) clearly shows that electron-phonon scattering processes in a quantum kinetic theory are nonlocal in space: By means of the operator $\hat{\mathbf{W}}^{\sigma\sigma'}$ it involves convolutions of the Wigner functions both in momentum and real space. However, it is difficult to get a deeper insight into this nonlocality of scattering processes from the full set of equations of motion for the two-band system including arbitrary inhomogeneities, because all the different sources of inhomogeneities are mixed together. In order to take a closer look on the nonlocality of scattering processes it is therefore convenient to concentrate on a simplified system. Therefore for the remaining part of this section we will restrict ourselves to the case of a single electron band without any space-dependent single-particle potentials. Furthermore we assume, as usual, a quadratic dispersion $\epsilon_{\mathbf{k}} = \hbar^2 \mathbf{k}^2/(2m_e)$ and we will consider the low-density limit where all phase-space filling factors $(1-\mathcal{F})$ can be replaced by unity. Due to the quadratic dispersion the operator $\hat{\mathbf{W}}^{\sigma\sigma'}$ in the parts involving energies effectively reduces to a first-order differential operator while in the source terms for the phonon-assisted density matrix only the zeroth order, i.e., the unity operator remains. Then, the coupled electron-phonon system is described by the set of equations of motion

$$\frac{\partial}{\partial t}\mathcal{F}^e_{\mathbf{k}}(\mathbf{r},t) = -\frac{\hbar \mathbf{k}}{m_e} \cdot \frac{\partial}{\partial \mathbf{r}} \mathcal{F}^e_{\mathbf{k}}(\mathbf{r},t) + \sum_{\mathbf{q}} 2\,\mathrm{Re}[\mathcal{S}^e_{\mathbf{k},\mathbf{q}}(\mathbf{r},t) - \mathcal{S}^e_{\mathbf{k}-\mathbf{q},\mathbf{q}}(\mathbf{r},t)], \tag{36a}$$

$$\frac{\partial}{\partial t}\mathcal{S}^e_{\mathbf{k},\mathbf{q}}(\mathbf{r},t) = \frac{i}{\hbar}(\epsilon_{\mathbf{k}+\mathbf{q}} - \epsilon_{\mathbf{k}} - \hbar\omega_{LO})\mathcal{S}^e_{\mathbf{k},\mathbf{q}}(\mathbf{r},t) - \frac{\hbar}{m_e}\left(\mathbf{k}+\frac{1}{2}\mathbf{q}\right)\cdot\frac{\partial}{\partial \mathbf{r}}\mathcal{S}^e_{\mathbf{k},\mathbf{q}}(\mathbf{r},t) + \frac{|g_{\mathbf{q}}|^2}{\hbar^2}[(n_{\mathbf{q}}+1)\mathcal{F}^e_{\mathbf{k}+\mathbf{q}}(\mathbf{r},t) - n_{\mathbf{q}}\mathcal{F}^e_{\mathbf{k}}(\mathbf{r},t)]. \tag{36b}$$

Equation (36b) can easily be solved formally resulting in

$$\begin{aligned}\mathcal{S}^e_{\mathbf{k},\mathbf{q}}(\mathbf{r},t) = {} & e^{(i/\hbar)(\epsilon_{\mathbf{k}+\mathbf{q}} - \epsilon_{\mathbf{k}} - \hbar\omega_{LO})(t-t_0)} \\ & \times \mathcal{S}^e_{\mathbf{k},\mathbf{q}}\left[\mathbf{r} - \frac{\hbar}{m_e}\left(\mathbf{k}+\frac{1}{2}\mathbf{q}\right)(t-t_0), t_0\right] \\ & + \frac{|g_{\mathbf{q}}|^2}{\hbar^2}\int_0^{t-t_0} d\tau\; e^{(i/\hbar)(\epsilon_{\mathbf{k}+\mathbf{q}} - \epsilon_{\mathbf{k}} - \hbar\omega_{LO})\tau} \\ & \times \left\{(n_{\mathbf{q}}+1)\mathcal{F}^e_{\mathbf{k}+\mathbf{q}}\left[\mathbf{r} - \frac{\hbar}{m_e}\left(\mathbf{k}+\frac{1}{2}\mathbf{q}\right)\tau, t-\tau\right]\right. \\ & \left. - n_{\mathbf{q}}\mathcal{F}^e_{\mathbf{k}}\left[\mathbf{r} - \frac{\hbar}{m_e}\left(\mathbf{k}+\frac{1}{2}\mathbf{q}\right)\tau, t-\tau\right]\right\}\end{aligned} \tag{37}$$

which in turn can be inserted into Eq. (36a) resulting in a closed integrodifferential equation for the electron Wigner function. Although the action of the operator $\hat{\mathbf{W}}^{\sigma\sigma'}$ did reduce to a unity operation, the resulting scattering kernel is still nonlocal in space. Here, the spatial nonlocality exclusively results from the drift operator $[\sim(\mathbf{k}+\frac{1}{2}\mathbf{q})\cdot(\partial/\partial\mathbf{r})]$ in Eq. (36b). Furthermore, it is clearly seen that the temporal and spatial nonlocality are intimately related; both involve the same integration variable τ.

D. Markov limits

The quantum kinetic approach as discussed in this paper takes into account the finite duration of a scattering process and the corresponding energy-time uncertainty. On the level of single-particle density matrices the dynamics is nonlocal in time; it involves a memory kernel as can be clearly seen, e.g., in Eq. (37). In a semiclassical kinetic theory, by means of a Markov approximation, memory effects are discarded

resulting in a dynamics of single-particle density matrices which is local in time. Such a Markov approximation, however, requires the specification of slowly varying functions. At this point the results become dependent on the selected basis because it is usually assumed that the diagonal elements in a given basis are slowly varying functions while the off-diagonal elements rotate with the corresponding energy difference. Physically, the assumption of slowly varying functions in the above sense implies that there is a distinguished basis of single-particle states such that the carrier dynamics before and after a scattering event evolves freely in time without interaction. In inhomogeneous systems, e.g., due to time-dependent self-consistent fields, it is not always clear which is the correct basis for the description of scattering processes. In this section we will discuss how different assumptions based on different representations lead to different dynamical equations. Transforming the results of different Markov-type approximations—which all neglect temporal nonlocalities—to the Wigner form allows us to perform a most conclusive comparison of the resulting differences with respect to spatial nonlocalities.

The Boltzmann limit for the electron-phonon scattering processes is obtained under the assumption that the Wigner function in Eq. (37) is a slowly varying function of τ when compared to the exponential function. Obviously, this requires both sufficiently slow temporal and spatial variations of the Wigner functions. In addition it is assumed that the system initially, i.e., at $t_0 \to -\infty$, was uncorrelated which corresponds to a vanishing phonon-assisted Wigner function. This Markov approximation then results in a phonon-assisted density matrix according to

$$\mathcal{S}^e_{\mathbf{k},\mathbf{q}}(\mathbf{r},t) = -\frac{\pi}{\hbar}|g_{\mathbf{q}}|^2 \mathcal{D}(\epsilon_{\mathbf{k}+\mathbf{q}} - \epsilon_{\mathbf{k}} - \hbar\omega_{LO}) \times [(n_{\mathbf{q}}+1)\mathcal{F}^e_{\mathbf{k}+\mathbf{q}}(\mathbf{r},t) - n_{\mathbf{q}}\mathcal{F}^e_{\mathbf{k}}(\mathbf{r},t)] \quad (38)$$

with

$$\mathcal{D}(x) = \frac{i}{\pi}\frac{\mathcal{P}}{x} + \delta(x). \quad (39)$$

When inserting this result into Eq. (36a), the imaginary parts of the function $\mathcal{D}$ cancel and the semiclassical Boltzmann equation with temporally and spatially local scattering processes is recovered.

However, it should be noted that one could also imagine situations where the assumption of a slowly varying dependence only holds for one of the two arguments. This holds, e.g., for a spatially slowly varying system excited by an ultrashort laser pulse where the spatial nonlocality is negligible but the temporal nonlocality results in typical quantum kinetic features like energy-time uncertainty. In this case the dynamics is similar to the quantum kinetics in homogeneous systems extended only by a parametric space dependence. Technically, this limit is obtained by neglecting the time-dependent displacement of the space arguments on the right-hand side of Eq. (37). On the other hand, in a temporally slowly varying system with sufficiently fast spatial variations the temporal retardation may be negligible but the nonlocality of the Wigner function has to be kept. This results in an instantaneous but spatially nonlocal scattering term according to

$$\mathcal{S}^e_{\mathbf{k},\mathbf{q}}(\mathbf{r},t) = \frac{|g_{\mathbf{q}}|^2}{\hbar^2}\int_0^\infty d\tau e^{(i/\hbar)(\epsilon_{\mathbf{k}+\mathbf{q}} - \epsilon_{\mathbf{k}} - \hbar\omega_{LO})\tau} \times \left\{ (n_{\mathbf{q}}+1)\mathcal{F}^e_{\mathbf{k}+\mathbf{q}}\left[\mathbf{r} - \frac{\hbar}{m_e}\left(\mathbf{k}+\frac{1}{2}\mathbf{q}\right)\tau, t\right] - n_{\mathbf{q}}\mathcal{F}^e_{\mathbf{k}}\left[\mathbf{r} - \frac{\hbar}{m_e}\left(\mathbf{k}+\frac{1}{2}\mathbf{q}\right)\tau, t\right]\right\}. \quad (40)$$

The basis for the derivation of Eq. (40) has been the assumption of a temporally slowly varying Wigner function. Another possibility which is often applied in problems involving off-diagonal density matrices is the Markov approximation in the original momentum representation.[36,37] By restricting ourselves again to the same one-band model discussed above, the exact formal solution for the phonon-assisted density matrix in $\mathbf{k}$ representation [Eq. (17)] is given by

$$s^e_{\mathbf{k}',\mathbf{q},\mathbf{k}}(t) = e^{(i/\hbar)(\epsilon_{\mathbf{k}'} - \epsilon_{\mathbf{k}} - \hbar\omega_{LO})(t-t_0)} s^e_{\mathbf{k}',\mathbf{q},\mathbf{k}}(t_0) + \frac{|g_{\mathbf{q}}|^2}{\hbar^2}\int_0^{t-t_0} d\tau e^{(i/\hbar)(\epsilon_{\mathbf{k}'} - \epsilon_{\mathbf{k}} - \hbar\omega_{LO})\tau} \times [(n_{\mathbf{q}}+1)f^e_{\mathbf{k}',\mathbf{k}+\mathbf{q}}(t-\tau) - n_{\mathbf{q}}f^e_{\mathbf{k}'-\mathbf{q},\mathbf{k}}(t-\tau)]. \quad (41)$$

In this representation it is natural to assume that the main time dependence of the single-particle density matrix is determined by the free-carrier Hamiltonian, i.e., $f^e_{\mathbf{k}',\mathbf{k}}(t) = \tilde{f}^e_{\mathbf{k}',\mathbf{k}}(t)\exp[(i/\hbar)(\epsilon_{\mathbf{k}'} - \epsilon_{\mathbf{k}})t]$ with a slowly varying function $\tilde{f}^e$. The Markov approximation now consists in neglecting the time dependence of $\tilde{f}^e$ when evaluating the integral. Considering again the limit $t_0 \to -\infty$ and assuming an uncorrelated initial condition, the resulting phonon-assisted density matrix can then be transformed into the Wigner representation which results in

$$\mathcal{S}^e_{\mathbf{k},\mathbf{q}}(\mathbf{r},t) = \frac{|g_{\mathbf{q}}|^2}{\hbar^2}\int_0^\infty d\tau e^{(i/\hbar)(\epsilon_{\mathbf{k}+\mathbf{q}} - \epsilon_{\mathbf{k}} - \hbar\omega_{LO})\tau}\left[(n_{\mathbf{q}}+1) \times \mathcal{F}^e_{\mathbf{k}+\mathbf{q}}\left(\mathbf{r} - \frac{\hbar\mathbf{q}}{2m_e}\tau, t\right) - n_{\mathbf{q}}\mathcal{F}^e_{\mathbf{k}}\left(\mathbf{r} + \frac{\hbar\mathbf{q}}{2m_e}\tau, t\right)\right]. \quad (42)$$

Because of the Markov approximation there is no temporal memory effect in Eq. (42). Nevertheless, the scattering processes exhibit a spatial nonlocality similar to Eq. (40). However, the time-dependent displacements of the space arguments are obviously different. This clearly shows that depending on the assumptions on slowly varying parts in the dynamics the spatial nonlocality of the scattering processes have different forms. Only if in addition the assumption of slowly varying spatial dependences is made the results of the

two types of Markov approximation coincide and lead to the same spatially local scattering processes as in the semiclassical Boltzmann equation.

III. RESULTS

After having introduced the theory we will now apply the quantum kinetic formalism to the study of the spatiotemporal dynamics on ultrafast time scales. In the general case of arbitrary inhomogeneities the single-particle density matrices depend on two **k** indices, i.e., they constitute six-dimensional variables. The phonon-assisted density matrices depend on three **k** indices and thus they constitute nine-dimensional dynamical variables. Even on a supercomputer this is clearly out of reach. The dimensions of the variables are reduced either if certain symmetries in the system and the excitation process are present or if, e.g., in nanostructured materials, the carrier system is confined in certain directions resulting in a dynamics in a lower dimensional space. Here we will apply the theory developed above to the dynamics in a cylindrical GaAs quantum wire with a 100-nm^2 cross section where the carriers are coupled via the Fröhlich interaction to three-dimensional bulk LO phonons. For this purpose we assume that the radial dependence of the electron and hole potential $V^{e,h}(\mathbf{r})$ is given by a potential well with infinite barriers and all radial dependences are projected onto the lowest subband wave function. This corresponds to replacing the Fröhlich and Coulomb interaction matrix elements by their projections according to

$$g^{(1D)}_{q_\parallel,q_\perp} = i\,\gamma_{\mathrm{ph}}\mathcal{G}(q_\perp)\frac{1}{\sqrt{q_\parallel^2+q_\perp^2}}, \tag{43a}$$

$$v^{(1D)}_{q_\parallel} = \frac{e^2}{\mathcal{V}\varepsilon_0\varepsilon_\infty}\sum_{\mathbf{q}_\perp}|\mathcal{G}(q_\perp)|^2\frac{1}{q_\parallel^2+q_\perp^2}, \tag{43b}$$

where $q_\parallel$ is the wave-vector component along the wire direction, $\mathbf{q}_\perp$ is the wave vector in the plane perpendicular to the wire,

$$\mathcal{G}(q_\perp) = \int |\psi(\mathbf{r}_\perp)|^2 e^{i\mathbf{q}_\perp\cdot\mathbf{r}_\perp} d^2r_\perp \tag{44}$$

is the form factor with $\psi(\mathbf{r}_\perp)$ being the lowest subband wave function given here by a Bessel function J_0. Then, all electronic wave vectors are one dimensional while the phonon wave vectors are three dimensional. We will present results both for a one-band model, where the relaxation of a given initial distribution allows us to concentrate on the quantum kinetic effects of the electron-phonon interaction, and for a two-band model, where carrier generation by means of an ultrashort laser pulse is explicitly taken into account. For all calculations a lattice temperature of 0 K has been assumed so that only phonon emission processes may occur. As has been stated above, we will concentrate on carrier-phonon scattering processes. Carrier-carrier interaction processes are accounted for on the mean-field level. This is a good approximation for sufficiently low-carrier densities as will be studied in most of the cases. Furthermore, it should be noted that in a one-dimensional system in the Markovian approximation electron-electron scattering processes may only exchange the momenta of the participating carriers and thus do not lead to a relaxation of the distribution functions. Therefore also in a quantum kinetic treatment carrier-carrier scattering in quantum wire structures may be expected to be strongly reduced when compared to higher dimensional systems.

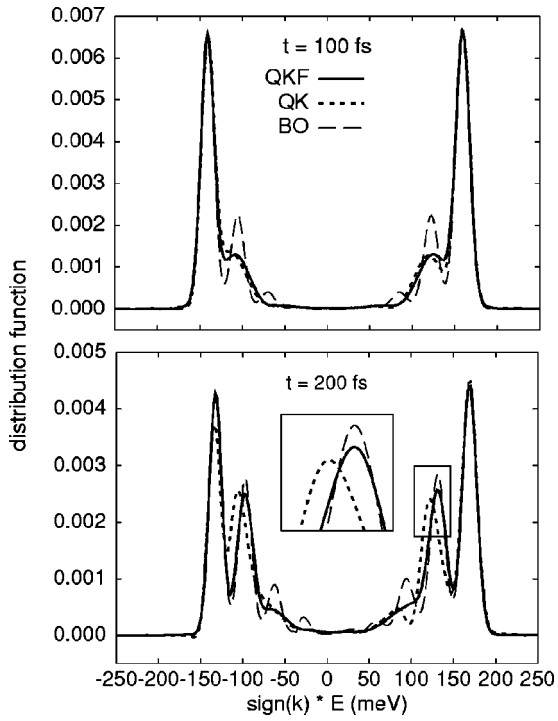

FIG. 1. Electron distribution functions as functions of energy at two different times showing the relaxation of an initially Gaussian distribution in the presence of a homogeneous electric field of $E=-1$ kV/cm. The different curves refer to the full quantum kinetic model with field (QKF), a quantum kinetic model where the effect of the field on the phonon-assisted density matrices has been neglected (QK), and a semiclassical Boltzmann model (BO).

A. Intracollisional field effect

Let us start by looking at the impact of a homogeneous static electric field on carrier relaxation. In order to concentrate on the relaxation process we will study the dynamics of an electron distribution function in a one-band model which is initially given by a Gaussian in energy centered around an excess energy of 150 meV. Figure 1 shows the electron distribution as a function of energy at two different times for the case of an electric field of $E=-1$ kV/cm. The calculations have been performed on three different levels of the theory: (i) the full quantum kinetic model (QKF) according to Eqs. (20a) and (22) where the field acts both on the distribution function and the phonon-assisted density matrix, a quantum kinetic model (QK) where the drift term in Eq. (22) has been neglected, and (iii) the semiclassical Boltzmann model with the usual field-independent scattering rates. It should be noted that the drift term in Eq. (22) represents the action of

the field ''during'' the carrier-phonon scattering process and is therefore the essence of the intracollisional field effect.

At $t=100$ fs we notice that the unrelaxed peaks have drifted by about 9 meV due to the acceleration by the electric field. We clearly see the strong broadening of the phonon replicas due to energy-time uncertainty in both quantum kinetic cases when compared to the Boltzmann case as it is well known from the relaxation in systems without electric field.[2] The two quantum kinetic cases exhibit slight differences, in particular in the energy ranges between the unrelaxed peaks and the first phonon replicas. At $t=200$ fs the drift of the unrelaxed peaks is about 18 meV. In the quantum kinetic cases now the replicas due to one phonon emission have essentially built up while the higher replicas are still considerably broadened. The most interesting feature, which is shown again in the inset on an enlarged scale, is the difference in the position of the peak maxima of the first phonon replicas. While the full quantum kinetic and the Boltzmann case exhibit a good agreement, the QK case where the drift term in the equation for the phonon-assisted density matrix has been neglected is considerably shifted. At first sight this behavior seems to be surprising because the Boltzmann scattering rates are obtained by neglecting the influence of the field on the scattering dynamics, i.e., a solution of Eq. (17) without the field term in the Markovian limit. However, it can be understood from the following argument: In a quantum kinetic treatment scattering processes take a finite time which is described by the dynamics of the phonon-assisted density matrices. During that time the carriers experience the action of the electric field expressed by the drift terms in the respective equations of motion. If this action of the field is neglected as in the case QK, the replicas build up at different energies. In the Boltzmann case, on the other hand, scattering processes are instantaneous events and therefore it is consistent to disregard the action of the field during the scattering process. For the case of a stationary distribution function this ''absence of the intracollisional field effect'' has also been discussed analytically.[53] In a quantum kinetic calculation which is relevant if the distribution functions are not slowly varying in time, however, it is essential to take into account the influence of the field on the scattering process, i.e., the intracollisional field effect.

B. Quantum kinetic scattering processes

After having studied the influence of a homogeneous electric field on the electron-phonon scattering process, in the following we will now investigate the quantum kinetics of spatially inhomogeneous carrier distributions. Such distributions may be generated, e.g., by means of a short-pulse optical excitation through the fiber tip of an optical near-field microscope.[27] The resulting distribution will then be characterized by a localization in k space determined by the excess energy and spectral shape of the laser pulse and a localization in real space determined by the electric-field profile resulting from the fiber tip. In order to concentrate on the quantum kinetics due to the electron-phonon interaction rather than the kinetics of the carrier generation process we first study the relaxation of an initial distribution which is

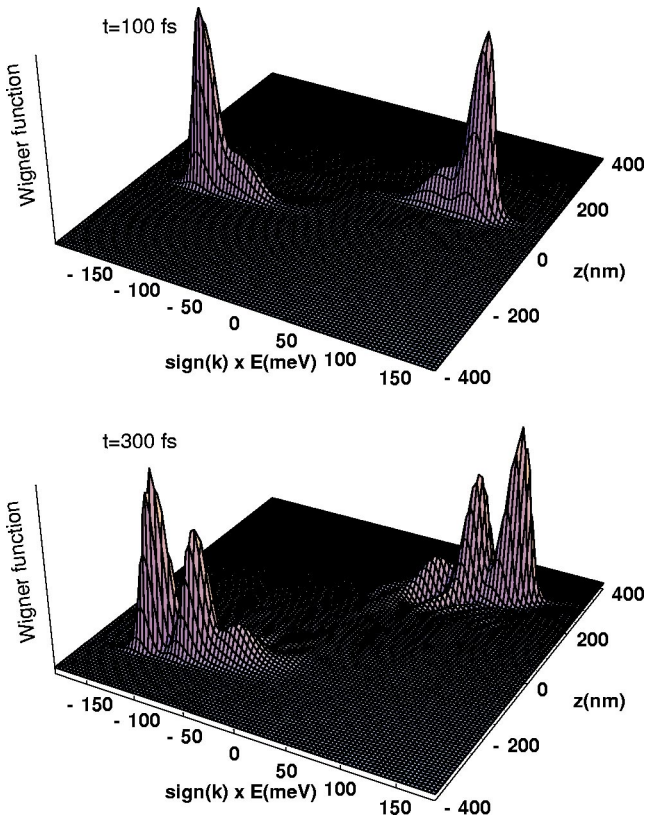

FIG. 2. Wigner function of electrons at two different times obtained from a quantum kinetic one-band model for the case of the relaxation of an initial Gaussian distribution in energy and space centered at 120 meV.

Gaussian both in energy and space coordinate in a one-band model. Then we will come to the more realistic case of a two-band model where carrier generation is accounted for in a fully coherent way.

Figure 2 shows the Wigner function for the case of an initial distribution with excess energy of 120 meV centered around $z=0$ at the times $t=100$ fs (upper part) and $t=300$ fs (lower part) as obtained from the quantum kinetic model. In Fig. 3 the corresponding results obtained from a solution of the semiclassical Boltzmann equation with the same initial condition are shown. The k dependence is plotted as a function of the energy $\hbar^2k^2/(2m)$, however, separately for positive and negative k values because this allows us to better interpret the phonon emission processes. With increasing time we see the motion of the positive k components in positive z direction and of the negative k components in negative z direction. In k direction we observe the buildup of the phonon replicas due to the emission of optical phonons. In the quantum kinetic case these replicas exhibit the well-known time-dependent broadening due to energy-time uncertainty as in the case of a spatially homogeneous excitation. At $t=100$ fs the first replica is strongly broadened; at $t=300$ fs this replica has become sharp while the second replica is still considerably broadened.

To analyze the kinetics in a more quantitative way, in Fig. 4 we have plotted the momentum distribution as well as the spatial profiles of the electron density, drift velocity, and

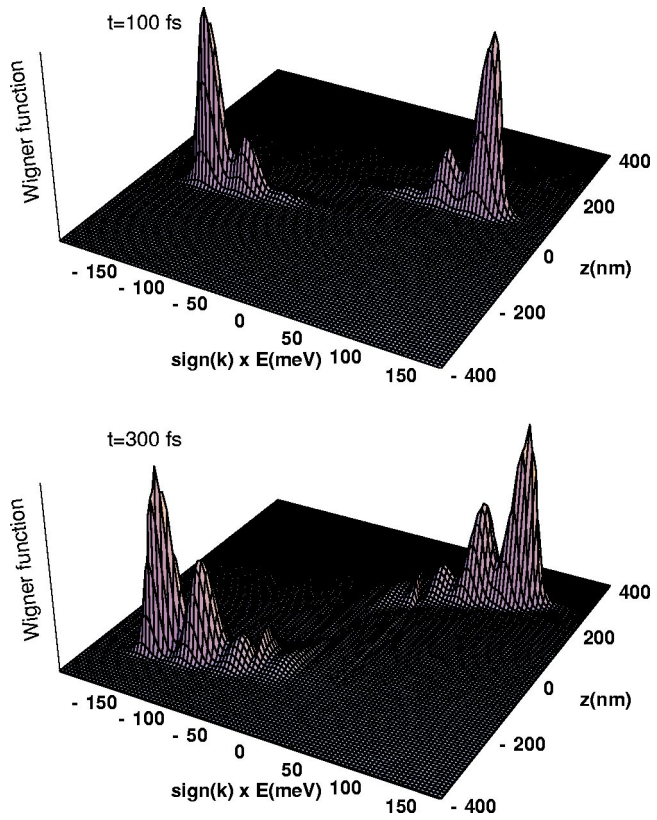

FIG. 3. Wigner function (distribution function) of electrons at two different times obtained from a semiclassical one-band model for the case of the relaxation of an initial Gaussian distribution in energy and space centered at 120 meV.

mean kinetic energy at the time $t=100$ fs which have been extracted from the Wigner function according to Eqs. (24) and (26). Here, in addition to the full quantum kinetic model (QK) and the Boltzmann model (BO) where carrier-phonon scattering processes are treated in the Markovian, spatially local limit we have included the completely ballistic dynamics (BAL) obtained from a calculation without any carrier-phonon interaction. It should be noted that the drift velocity and mean kinetic energy are only well defined at those positions where the density is essentially nonzero. In the ballistic case (BAL) momentum is a conserved quantity and consequently the momentum distribution is independent of time. The spatial distribution splits into two peaks moving outward with the drift velocity corresponding to the excess energy. The peaks remain approximately Gaussian. The profiles of the velocity and of the mean energy are slightly inclined because the leading edge of the peaks is formed by the carriers with higher energy and thus higher group velocity. In the Boltzmann case (BO) we clearly see the buildup of phonon replicas in the momentum distribution. Because we are at low temperatures, no phonon absorption is possible. Therefore the high-energy decay of the momentum distribution agrees with the ballistic case: no carriers have higher energies than without carrier-phonon interaction. This is reflected also in the spatial profiles. Also here the front edge of the carrier density coincides with the ballistic case and both the drift velocity and mean energy are always below the corresponding values of the ballistic model. The situation changes in the quantum kinetic case. In the momentum distribution energy-time uncertainty leads to the smearing of the phonon replicas inbetween the two ballistic peaks as already discussed above. However, with a small but clearly noticeable probability it also gives rise to transitions to higher energy states above the initial distribution. In the logarithmic plot we clearly see a nonvanishing contribution at energies above the initial distribution. They exhibit an oscillatory behavior which reflects the function $(1/\Delta E)\sin(\Delta E t/\hbar))$ which in the long-time limit reduces to the energy-conserving delta function. Indeed, the oscillation period in Fig. 4(c) is just $2\pi\hbar/100$ fs which is 41.4 meV. The high-momentum components reflect themselves also in the spatial profiles. Because of their higher group velocity those carriers move faster and therefore give rise to a contribution to the density ahead of the ballistic peaks. In these spatial regions the high-

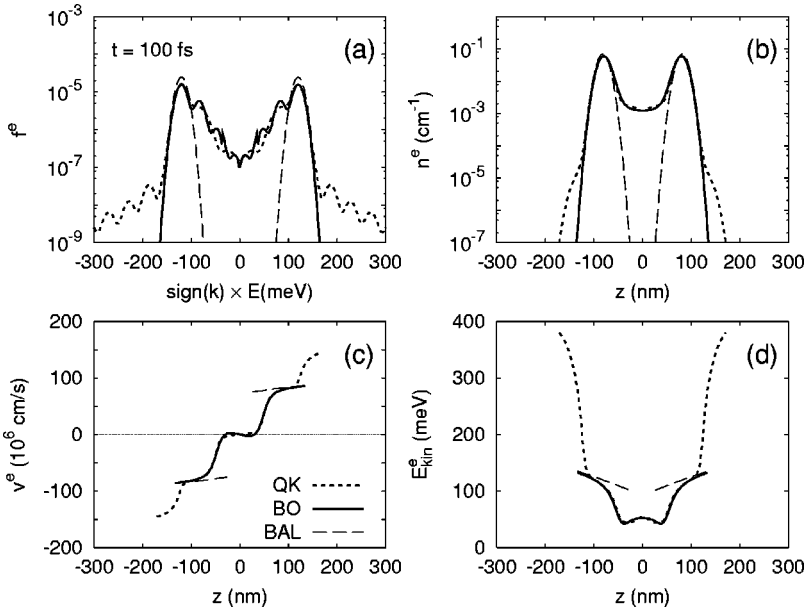

FIG. 4. (a) Momentum distribution, (b) electron density, (c) drift velocity, and (d) mean kinetic energy at the time $t=100$ fs in a one-band model corresponding to the Wigner functions in Figs. 2 (QK) and 3 (BO). The long-dashed lines refer to the ballistic case without carrier-phonon interaction (BAL).

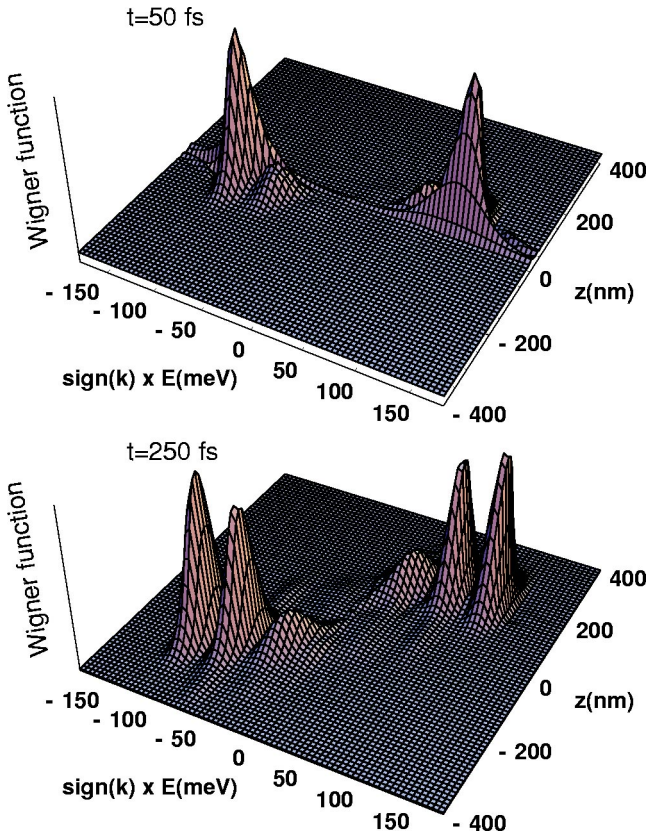

FIG. 5. Wigner function of electrons at two different times obtained from a quantum kinetic two-band model for the case of excitation by a 100-fs laser pulse with an excess energy of 120 meV.

momentum carriers dominate and therefore both the drift velocity and even more pronounced the mean kinetic energy assume values much higher than in the ballistic case.

The previous results have been obtained within a one-band model where we have studied the relaxation of a given initial distribution. Of course, such an initial distribution has to be created somehow. As already mentioned, the generation of a spatially localized carrier distribution may be realized by exciting the system by a short laser pulse through the tip of a near-field microscope. To take into account this generation process we now consider the full two-band model where the laser excitation is modeled by an electric field amplitude which is Gaussian both in time and space. Figure 5 shows the resulting Wigner function of electrons at two different times for the case of excitation by a 100-fs laser pulse peaked at $t=0$. As can be seen by comparing Figs. 5 and 2, the times 50 and 250 fs in the two-band model correspond roughly to the times 100 and 300 fs in the one-band case with initial condition. At $t=50$ fs the laser has been acting on the system roughly ~ 100 fs but the pulse is not yet completed. Therefore in addition to the broadening of the phonon replica we observe the time-dependent broadening of the photogenerated peaks resulting from the coherent dynamics of the interband polarization.[66–68] At $t=250$ fs the pulse is finished. The generated peak and the first phonon replica have essentially reached their final width while, as in the one-band case, the second replica still exhibits a considerable broadening. This clearly demonstrates that, as can be expected, the typical quantum kinetic features of carrier-phonon interaction are the same in the one-band and the two-band model. In the latter, however, additional features related to the dynamics of the polarization and, in principle, also to the dynamics of the hole distribution are superimposed. This justifies the use of the simpler one-band case to concentrate on the quantum kinetics of electron-phonon interaction. The quantitative modeling of a realistic experimental situation of course requires a two-band model.

C. Coherent phonon dynamics

Spatially inhomogeneous carrier distributions where electron and hole distributions do not exactly coincide are sources for an internal electric field which, by means of the Fröhlich interaction, acts on the ions in a polar crystal and leads to the generation of coherent phonons.[69–73] Such a situation is realized in the scenarios studied in the previous section where carriers have been generated locally in space with a given excess energy. In this section we will study the dynamics of coherent phonons which are excited by the electron and hole distributions according to Eq. (13). We will again consider both a one-band model with given initial distribution and a two-band model including carrier photogeneration. In order to satisfy overall charge neutrality, which is necessary to obtain reasonable results, the initial distribution in the one-band model has been compensated by a hole distribution assuming, however, an infinite hole mass so that the holes do not move. The initial spatial distributions of electrons and holes have been chosen to be identical. We first concentrate on the coherent phonons by switching off all contributions due to incoherent phonons (i.e., all phonon-assisted density matrices are switched off) and then take into account also the incoherent phonons.

In Fig. 6 we have plotted the z component of the lattice polarization along the axis of the quantum wire (solid lines) obtained at three different times in the one-band (left column) and two-band (right column) model without incoherent phonon contributions. The excess energy of the electrons is again 120 meV as in the previous section. The dashed lines display the charge density due to electrons and holes. Here we have chosen a low-density condition such that the self-energy contributions due to Hartree and coherent phonon terms [Eq. (18a)] are negligible. Then, in the absence of incoherent phonon parts the carriers move ballistically. In the one-band model the density profiles of the electrons slightly spread due to the free-carrier dispersion relation while the holes with their infinite mass remain fixed. Inbetween the two electronic peaks in the charge density we clearly notice a spatially oscillating lattice polarization. The physical origin of this behavior can be understood as follows: As the electrons pass by some point in space, they nearly instantaneously switch on an electric field at this point. This leads to new equilibrium positions of the lattice ions and, due to the fast switching, the ions start to oscillate with the LO phonon frequency around this new equilibrium position. The motion of the electronic wave packet then translates this temporal oscillation also in a spatial oscillation. Being a quasi-one-

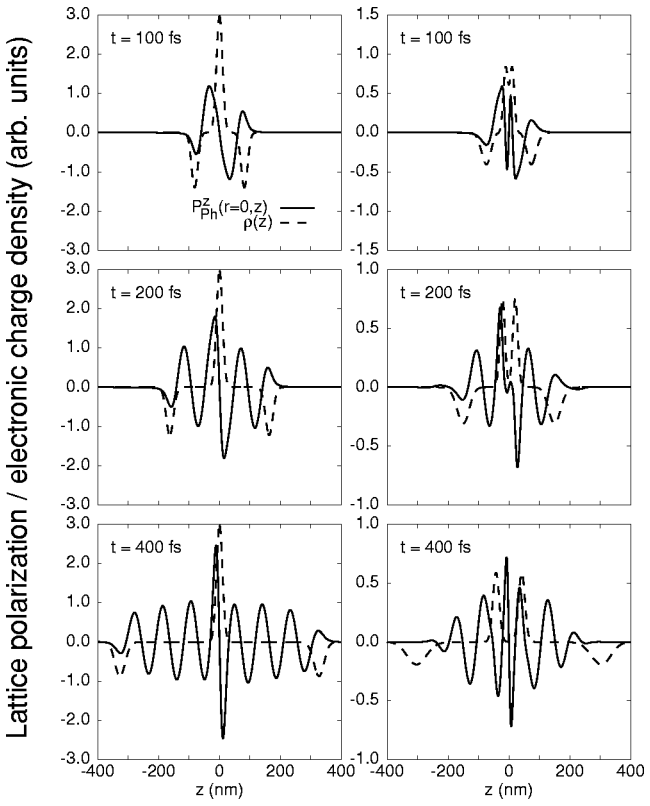

FIG. 6. Lattice polarization (solid lines) and electronic charge densities (dashed lines) along the wire axis at three different times obtained for the dynamics of a Gaussian initial distribution of electrons and holes with holes of an infinite effective mass (left panel) and for the dynamics of electrons and holes generated by a 100-fs laser pulse with an excess energy of 120 meV (right panel). Incoherent phonon dynamics has been switched off.

dimensional system, the electric field between electrons and holes decreases with increasing distance. This leads to a slight reduction of the oscillation amplitude with increasing distance from the origin. The right column in Fig. 6 shows the charge densities and the lattice polarization obtained in a full two-band model with finite hole mass where the carrier generation by a 100-fs laser pulse has been taken into account. The finite duration of the generation process leads to an additional spatial broadening mainly of the electron distribution, the finite hole mass leads to a motion also of the positive charge density. Qualitatively we find the same behavior as in the one-band model, however, the spatial profiles are more complicated due to the motion of the holes. When the holes pass by a given point they again change the electric field which gives rise to an additional kick on the lattice ions. Because of the slower motion of the holes the resulting spatial profile exhibits a smaller period than after the electronic excitation.

The electric field created by the electrons and holes is not restricted to the quantum wire. Therefore also coherent phonon amplitudes are not only excited in the wire region, they also extend into the barrier regions. Figure 7 shows the full spatial profile of the z component [Fig. 7(a)] and the radial component [Fig. 7(b)] of the lattice polarization at $t = 200$ fs for the one-band case discussed above. The radius

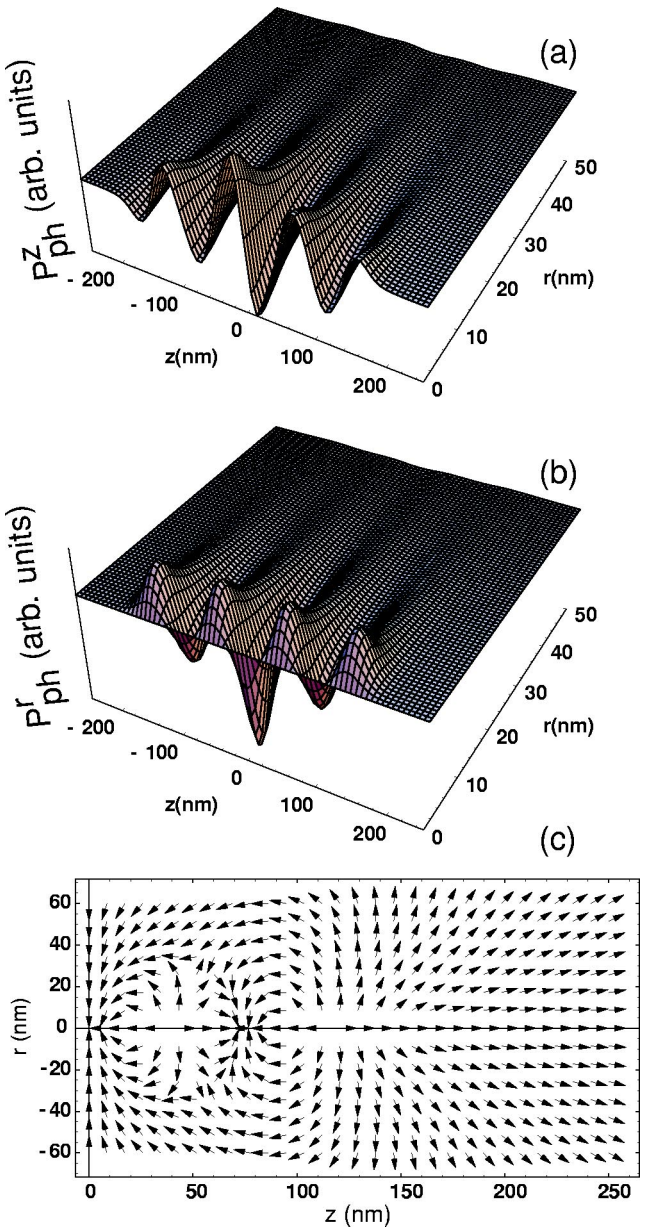

FIG. 7. Lattice polarization as a function of longitudinal (z) and radial (r) coordinate at the time $t = 200$ fs obtained for the dynamics of a Gaussian initial distribution of electrons and infinite-mass holes. (a) z component, (b) r component, and (c) direction field.

of the quantum wire is about 5.6 nm; thus we find that the phonon amplitudes extend to several times the radius into the barrier regions. As required by symmetry, on the wire axis the lattice polarization has only a z component. If we move away from the axis, the polarization also acquires a radial component. The different shapes of the radial and longitudinal components already indicate a nontrivial space dependence of the complete vector field $\mathbf{P}_{\mathrm{ph}}$. This is shown in Fig. 7(c) where we have plotted the corresponding directional field of the polarization vector. It turns out that away from the wire axis the lattice ions perform a quite complicated motion because here also the direction of the electric field associated with the moving charges changes with time.

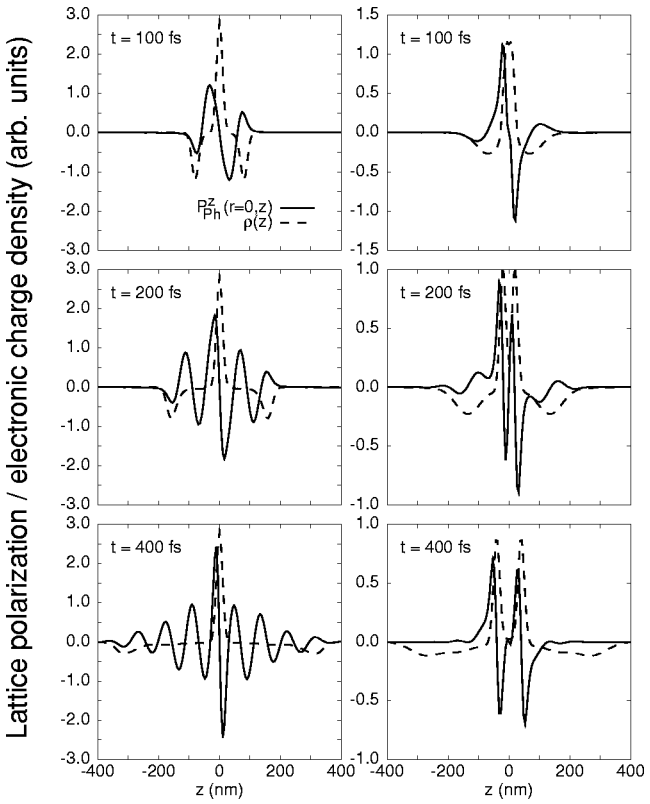

FIG. 8. Same as Fig. 6 but including incoherent phonon dynamics.

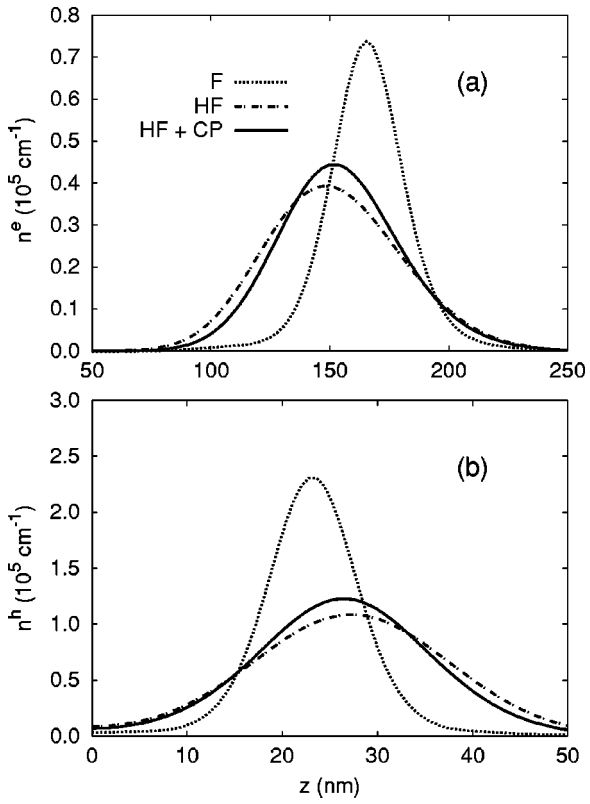

FIG. 9. Spatial profile of (a) electron and (b) hole density at the time $t=400$ fs for the case of carriers generated by a 100-fs laser pulse with an excess energy of 30 meV. Incoherent phonon dynamics has been switched off. The curves refer to calculations taking into account Fock terms (F), Hartree and Fock terms (HF), as well as additionally coherent phonons (HF+CP).

Taking into account the incoherent phonon contributions leads to an additional spatial broadening because now the carriers do not anymore move ballistically. The consequences for the dynamics of coherent phonons is shown in Fig. 8 where the lattice polarization (solid lines) and charge density (dashed lines) are plotted again for the one-band (left column) and two-band model (right column) now including incoherent phonons. The carriers which have emitted one or several optical phonons are slower and therefore accumulate inbetween the two ballistic peaks. Therefore the carrier density in the ballistic peak decreases with increasing time resulting in a reduced switching-on of the electric field. As can be seen, in particular in the one-band case (left column) this leads to an effective spatial damping of the coherent phonon oscillations. In the two-band case this behavior is even much more pronounced because here, as already mentioned above, the finite generation time leads to a spatial broadening during the generation and also the phonon emission already starts during the generation which leads again to an increased broadening. This leads to much smaller time derivatives of the induced electric field and thus to a strongly reduced excitation of coherent phonons. The region with considerable lattice polarization is here essentially confined to the region where the carriers have been generated.

D. Phononic screening

As has been discussed in the previous section, space- and time-dependent electronic charge densities in polar semiconductors excite coherent phonon amplitudes. These amplitudes, in turn, affect the dynamics of electrons and holes since they enter in the energy matrices according to Eq. (18a). In this section we will analyze in more detail this feedback mechanism.

The excitation of coherent phonons is proportional to the carrier density [see Eq. (18a)], therefore also the feedback on the carrier dynamics will depend on the density. Since also the Hartree and intraband Fock terms are linear in the carrier densities, these contributions will be of the same order as the coherent phonon contribution. In the previous sections we have always restricted ourselves to the low-density limit where the influence of coherent phonons and Hartree-Fock terms on the carrier dynamics (except for the Coulomb enhancement in the generation process) has been negligible. Now we will consider the excitation of a spatially localized electron-hole distribution with a higher density where these terms will come into play.

In Fig. 9 we have plotted the electron [part (a)] and hole density [part (b)] at the time $t=400$ fs for the case of excitation with a 100-fs laser pulse at an excess energy of 30 meV. In order to concentrate on the effects of coherent phonons and Hartree-Fock terms incoherent phonon contributions have been neglected in these calculations. The curves refer to different levels of the theory [see Eq. (18a)]: For the dotted lines only the Fock terms in the dynamics have been

included. Physically this corresponds to taking into account Coulomb enhancement and band-gap renormalization. We see essentially a ballistic motion of the carriers. Due to their much higher effective mass the holes are generated with a much lower group velocity and consequently they travel much slower. If we now switch on the Hartree terms (dash dotted lines) the carriers experience the repulsion due to the effective field created by the carriers of the same sort as well as the attraction due to the field created by the carriers of opposite charge. As a result of the repulsion we find a considerable broadening of the spatial profiles of electron and hole density. In addition, the maxima are shifted due to the attractive forces: The holes are accelerated by the faster moving electrons while the electrons are slowed down by the holes. The solid lines finally refer to a calculation where besides Hartree and Fock terms also the coherent phonon contributions have been included. We can clearly see that they reduce the influence of the Hartree terms by reducing both the broadening and the shift of the maxima. This already points to the interpretation that here the field created by the coherent phonons screens the interaction among the carriers.

To get more insight into this phenomenon, Fig. 10 shows for two different times the self-consistent potential in Wigner representation for the electrons $V^e_{\rm sc}(z) = -e\Phi_{\rm sc}(z)$ along the wire axis [Eq. (34a)] which is equivalent to the solution of the Poisson equation [Eq. (35)]. The corresponding potential for the holes is simply $V^h_{\rm sc}(z) = e\Phi_{\rm sc}(z) = -V^e_{\rm sc}(z)$. The Hartree contribution (dotted lines) exhibits maxima at the position of the electrons which give rise to the broadening of the density profile and minima at the position of the holes which lead to the slowing down of the motion of the electrons. The coherent phonon contribution (dashed lines) exhibits essentially the same shape as the Hartree contribution, however, with the opposite sign and a smaller amplitude giving rise to a total potential (solid curve) which is indeed a screened Hartree potential. We want to point out that the phonon oscillation time $2\pi/\omega_{LO} \approx 115$ fs is just of the same order as the spatial dynamics of the electron-hole system, thus the lattice displacement does not adiabatically follow the motion of electrons and holes as has been seen also in the previous section. The calculations including coherent phonon amplitudes, however, describe the phononic screening of external as well as of Hartree potentials in a fully dynamical way.

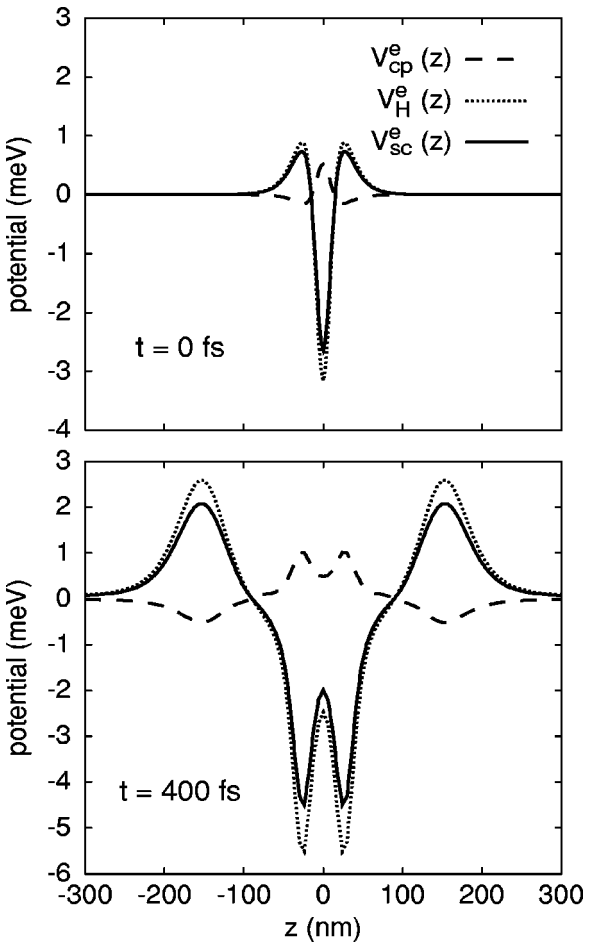

FIG. 10. Self-consistent potential for electrons at two different times for the same parameters as in Fig. 9. The curves refer to the Hartree contribution (V^e_H), the coherent phonon contribution (V^e_{cp}), and the total self-consistent potential (V^e_{sc}).

IV. CONCLUSIONS

In this paper we have presented a systematic analysis of the role of carrier-phonon interaction for the ultrafast carrier dynamics in photoexcited semiconductors in the presence of spatial inhomogeneites. For this purpose we have extended the density-matrix formalism for electron-phonon interaction which has been previously used for the study of spatially homogeneous systems to include arbitrary space dependences both in the semiconductor structure and in the photoexcitation process. A natural consequence in the correlation expansion is the appearance of coherent phonon amplitudes in the first order of the correlation expansion. The second order then gives rise to incoherent phonon contributions like phonon emission and absorption processes. By transforming the resulting equations of motion into the Wigner representation we have clearly identified the spatial nonlocality which turned out to be intimately related to the temporal nonlocality. Different Markov-type approximations based on different assumptions concerning the slowly varying parts of the dynamical variables give rise to different forms of the spatial nonlocality.

The theory has been applied to the dynamics of the carrier-phonon system after excitation with a short optical pulse. In the presence of a static electric field it turned out to be essential to include the drift in k space also in the scattering dynamics if, as is done in the quantum kinetic approach, the finite collision duration is taken into account. In the case of excitation of a localized electron and/or hole wave packet we have seen in the k-space dynamics typical quantum kinetic features like energy-time uncertainty as they are well known in homogeneous systems. Here, however, they also modify the spatial dynamics because of the population of high-energetic k states which are not occupied in the semiclassical limit. The charge densities created by the drifting

and relaxing wave packets excite coherent phonon oscillations which are effectively damped by the phonon emission processes because these processes lead to a strong spatial broadening of the charge density and therefore reduce the electric field responsible for the displacement of the lattice ions. Coherent phonons screen the Coulomb interaction between the carriers. The quantum kinetic approach describes this screening in a fully dynamical way.

ACKNOWLEDGMENT

This work has been partially supported by the Deutsche Forschungsgemeinschaft within the Schwerpunktprogramm Quantenkohärenz in Halbleitern and within the Graduiertenkolleg Nichtlineare kontinuierliche Systeme as well as by the European Commission through the TMR network Ultrafast Quantum Optoelectronics.

[1] D.B. Tran Thoai and H. Haug, Phys. Rev. B **47**, 3574 (1993).
[2] J. Schilp, T. Kuhn, and G. Mahler, Phys. Rev. B **50**, 5435 (1994).
[3] J.A. Kenrow, Phys. Rev. B **55**, 7809 (1997).
[4] C. Fürst, A. Leitenstorfer, A. Laubereau, and R. Zimmermann, Phys. Rev. Lett. **78**, 3733 (1997).
[5] K. Hannewald, S. Glutsch, and F. Bechstedt, Phys. Rev. B **61**, 10 792 (2000).
[6] L. Bányai, D.B. Tran Thoai, E. Reitsamer, H. Haug, D. Steinbach, M.U. Wehner, M. Wegener, T. Marschner, and W. Stolz, Phys. Rev. Lett. **75**, 2188 (1995).
[7] M.U. Wehner, D.S. Chemla, and M. Wegener, Phys. Rev. B **58**, 3590 (1998).
[8] U. Woggon, F. Gindele, W. Langbein, and J.M. Hvam, Phys. Rev. B **61**, 1935 (2000).
[9] M.U. Wehner, M.H. Ulm, D.S. Chemla, and M. Wegener, Phys. Rev. Lett. **80**, 1992 (1998).
[10] D. Steinbach, G. Kocherscheidt, M.U. Wehner, H. Kalt, M. Wegener, K. Ohkawa, D. Hommel, and V.M. Axt, Phys. Rev. B **60**, 12 079 (1999).
[11] V.M. Axt, M. Herbst, and T. Kuhn, Superlattices Microstruct. **26**, 117 (1999).
[12] V.M. Axt, K. Siantidis, M. Herbst, T. Kuhn, S. Grosse, M. Koch, and J. Feldmann, Mater. Sci. Forum **297-298**, 79 (1999).
[13] N. Donlagic and T. Östreich, Phys. Rev. B **59**, 7493 (1999).
[14] W. Schäfer, J. Opt. Soc. Am. B **13**, 1291 (1996).
[15] F.X. Camescasse, A. Alexandrou, D. Hulin, L. Bányai, D.B. Tran Thoai, and H. Haug, Phys. Rev. Lett. **77**, 5429 (1996).
[16] W.A. Hügel, M.F. Heinrich, M. Wegener, Q.T. Vu, L. Bányai, and H. Haug, Phys. Rev. Lett. **83**, 3313 (1999).
[17] L. Bányai, Q.T. Vu, B. Mieck, and H. Haug, Phys. Rev. Lett. **81**, 882 (1998).
[18] P. Gartner, L. Bányai, and H. Haug, Phys. Rev. B **62**, 7116 (2000).
[19] M. Bonitz, J.F. Lampin, F.X. Camescasse, and A. Alexandrou, Phys. Rev. B **62**, 15 724 (2000).
[20] N.-H. Kwong and M. Bonitz, Phys. Rev. Lett. **84**, 1768 (2000).
[21] T. Wolterink, V.M. Axt, and T. Kuhn, Physica B **314**, 132 (2002).
[22] Q.T. Vu, H. Haug, W.A. Hügel, S. Chatterjee, and M. Wegener, Phys. Rev. Lett. **85**, 3508 (2000).
[23] E. Betzig, J.K. Trautmann, T.D. Harris, J.S. Weiner, and R.L. Kostelak, Science **251**, 1468 (1991).
[24] A. Naber, D. Molenda , U.C. Fischer, H.-J. Maas, C. Höppener, N. Lu, and H. Fuchs, Phys. Rev. Lett. **89**, 210801 (2002).
[25] V. Emiliani, T. Günther, F. Intonti, A. Richter, C. Lienau, and T. Elsaesser, J. Phys.: Condens. Matter **11**, 5889 (1999).
[26] C. Lienau, V. Emiliani, T. Guenther, F. Intonti, T. Elsaesser, R. Nötzel, and K.H. Ploog, Phys. Status Solidi A **178**, 471 (2000).
[27] T. Guenther, C. Lienau, T. Elsaesser, M. Glanemann, V.M. Axt, T. Kuhn, S. Eshlaghi, and A.D. Wieck, Phys. Rev. Lett. **89**, 057401 (2002).
[28] U. Neuberth, L. Waller, G. von Freymann, B. Dal Don, H. Kalt, M. Wegener, G. Khitrova, and H.M. Gibbs, Appl. Phys. Lett. **80**, 3340 (2002).
[29] B. Dal Don, R. Dianoux, S. Wachter, E. Kurtz, G. von Freymann, U. Neuberth, C. Klingshirn, M. Wegener, and H. Kalt, Phys. Status Solidi A **190**, 533 (2002).
[30] M. Vollmer, H. Giessen, W. Stolz, W.W. Rühle, L. Ghislain, and V. Elings, Appl. Phys. Lett. **74**, 1791 (1999).
[31] H. Zhao, S. Moehl, S. Wachter, and H. Kalt, Appl. Phys. Lett. **80**, 1391 (2002).
[32] D. Gammon, E.S. Snow, B.V. Shanabrook, D.S. Katzer, and D. Park, Phys. Rev. Lett. **76**, 3005 (1996).
[33] C. Sönnichsen, A.C. Duch, G. Steininger, M. Koch, G. von Plessen, and J. Feldmann, Appl. Phys. Lett. **76**, 140 (2000).
[34] J. Hetzler, A. Brunner, M. Wegener, S. Leu, S. Nau, and W. Stolz, Phys. Status Solidi B **221**, 425 (2000).
[35] A. von der Heydt, A. Knorr, B. Hanewinkel, and S.W. Koch, J. Chem. Phys. **112**, 7831 (2000).
[36] F. Steininger, A. Knorr, P. Thomas, and S.W. Koch, Z. Phys. B: Condens. Matter **103**, 45 (1997).
[37] A. Knorr, F. Steininger, B. Hanewinkel, S. Kuckenburg, P. Thomas, and S.W. Koch, Phys. Status Solidi B **206**, 139 (1998).
[38] J. Schilp, T. Kuhn, and G. Mahler, Phys. Status Solidi B **188**, 417 (1995).
[39] T. Kuhn, in *Theory of Transport Properties of Semiconductor Nanostructures*, edited by E. Schöll (Chapman and Hall, London, 1998), p. 173.
[40] O. Madelung, *Introduction to Solid-State Theory* (Springer, Berlin, 1978).
[41] C. Cohen-Tannoudji, J. Dupont-Roc, and G. Grynberg, *Photons and Atoms* (Wiley, New York, 1989).
[42] M. Kira, F. Jahnke, W. Hoyer, and S.W. Koch, Prog. Quantum Electron. **23**, 189 (1999).
[43] J. Sak, Phys. Rev. Lett. **25**, 1654 (1970).
[44] I.B. Levinson, Sov. Phys. JETP **30**, 362 (1970).
[45] J.R. Barker, J. Phys.: Condens. Matter **6**, 2663 (1973).
[46] J.R. Barker and D.K. Ferry, Phys. Rev. Lett. **42**, 1779 (1979).
[47] A.P. Jauho, Phys. Rev. B **32**, 2248 (1985).
[48] F.S. Khan, J.H. Davies, and J.W. Wilkins, Phys. Rev. B **36**, 2578 (1987).
[49] L. Reggiani, P. Lugli, and A.P. Jauho, Phys. Rev. B **36**, 6602 (1987).
[50] R. Brunetti, C. Jacoboni, and F. Rossi, Phys. Rev. B **39**, 10 781 (1989).

[51] R. Bertoncini, A.M. Kriman, and D.K. Ferry, Phys. Rev. B **41**, 1390 (1990).
[52] R. Bertoncini and A.P. Jauho, Phys. Rev. B **44**, 3655 (1991).
[53] P. Lipavský, F.S. Khan, F. Abdolsalami, and J.W. Wilkins, Phys. Rev. B **43**, 4885 (1991).
[54] J. Hader, T. Meier, S.W. Koch, F. Rossi, and N. Linder, Phys. Rev. B **55**, 13 799 (1997).
[55] T.V. Gurov, M. Nedjalkov, P.A. Whitlock, H. Kosina, and S. Selberherr, Physica B **314**, 301 (2002).
[56] M. Herbst, V.M. Axt, T. Kuhn, and J. Schilp, Phys. Status Solidi B **204**, 358 (1997).
[57] E. Wigner, Phys. Rev. **40**, 749 (1932).
[58] U. Ravaioli, M.A. Osman, W. Pötz, N. Kluksdahl, and D.K. Ferry, Physica B **134**, 36 (1985).
[59] W.R. Frensley, Phys. Rev. Lett. **57**, 2853 (1986).
[60] N.C. Kluksdahl, A.M. Kriman, D.K. Ferry, and C. Ringhofer, Phys. Rev. B **39**, 7720 (1989).
[61] W.R. Frensley, Rev. Mod. Phys. **62**, 745 (1990).
[62] R. Brunetti and C. Jacoboni, Phys. Rev. B **57**, 1723 (1998).
[63] P. Bordone, M. Pascoli, R. Brunetti, A. Bertoni, C. Jacoboni, and A. Abramo, Phys. Rev. B **59**, 3060 (1999).
[64] L. Demeio, L. Barletti, A. Bertoni, P. Bordone, and C. Jacoboni, Physica B **314**, 104 (2002).
[65] O. Hess and T. Kuhn, Phys. Rev. A **54**, 3347 (1996).
[66] T. Kuhn and F. Rossi, Phys. Rev. B **46**, 7496 (1992).
[67] F. Rossi, S. Haas, and T. Kuhn, Phys. Rev. Lett. **72**, 152 (1994).
[68] A. Leitenstorfer, A. Lohner, T. Elsaesser, S. Haas, F. Rossi, T. Kuhn, W. Klein, G. Boehm, G. Traenkle, and G. Weimann, Phys. Rev. Lett. **73**, 1687 (1994).
[69] G.C. Cho, W. Kütt, and H. Kurz, Phys. Rev. Lett. **65**, 764 (1990).
[70] T. Pfeifer, W. Kütt, H. Kurz, and R. Scholz, Phys. Rev. Lett. **69**, 3248 (1992).
[71] R. Scholz, T. Pfeifer, and H. Kurz, Phys. Rev. B **47**, 16 229 (1993).
[72] A.V. Kuznetsov and C.J. Stanton, Phys. Rev. Lett. **73**, 3243 (1994).
[73] T. Dekorsy, G. C. Cho, and H. Kurz, in *Light Scattering in Solids VIII*, edited by M. Cardona and G. Güntherodt (Springer, Berlin, 2000), p. 169.